Erosion in Bedrock and Alluvial Meanders through 2 Dimensional Numerical Models, Laboratory Experiments and Field Observations

岩盤河床河岸河川および沖積地河川における河岸侵食と蛇行に関する研究

By

Jagriti Mishra

A thesis submitted in partial fulfillment of the requirements for the degree of Doctor of Philosophy in Engineering

Under the guidance of
Professor Yasuyuki Shimizu

Examination Committee:

Prof. Yasuyuki Shimizu
Prof. Norihiro Izumi
Prof. Yasunori Watanabe

Doctor's thesis

Hydraulics Research Laboratory
Division of Field Engineering for Environment
Graduate School of Engineering, Hokkaido University

September, 2017

ABSTRACT

Like alluvial rivers, Meandering is a phenomena common in Bedrock Rivers also. A major number of studies conducted to understand meandering phenomena have concentrated their focus on alluvial meandering [Parker 1976, 2011 and Asahi 2013]. The characteristics of meandering in alluvial and bedrock channels are noticeably different from one another. To expand our understanding of landscape formation, it is vital that we understand bedrock channel characteristics as well as alluvial channel characteristics.

In the first part of this thesis, an attempt has been made to understand the process of erosion in Bedrock meanders. Several laboratory scale experiments were conducted to understand the process of erosion in bedrock channels. The focus was on erosion caused due to abrading bedload in a bend. This is the first time an experimental study is performed in Bedrock bend. Multiple experiments were conducted to observe the changes occurring in a bedrock bend associated with changes in sediment flux. The experiments showed that vertical incision had a more complex relation with the sediment feed rate. A u-shaped channel roughly 1/1000 of the scale of Shimanto river was used to perform the experiments.

The relationship between sediment flux and vertical and lateral erosion in bedrock bend was stablished post multiple laboratory scale experiments and on-field observations. These relationships were numerically implemented and tested to produce desirable results. From this study, it was concluded that bank erosion is largely effected by sediment supply. It increases linearly with increase in sediment. It was also found that, bank erosion increases with increase in lateral bedslope, as effect of secondary flow decreases. Also, length and depth of bank erosion increased with increased sediment flux. We also observed the morphological differences in alluvial bend and bedrock bend. It was observed that bedrock bends largely erode in the center of the channel whereas alluvial bends are considered to largely erode in the outer bend of the channel.

Experiments were also conducted using a laboratory scale Sine Generated Curve channel to get a more explicit outlook regarding the effect of sediment on bedrock bends. It was observed that, erosion in bedrock banks is primarily caused by bedload. This study, combined with results of U-channel study, imply that sediment supply is a dominating factor causing erosion in bedrock banks.

Also, numerical model proposed by Inoue et al. (2015, Gravel bed river, 8) was established in this study. The model uses transverse bedload transfer rate in order to calculate bank erosion in bedrock channels. The model can successfully reproduce the laboratory scale experiments. Also, the model produced results in agreement with U-channel experiments, i.e. lateral erosion increases with increase in sediment feed rate, also, increased sediment feed shifts the start point of erosion towards the upstream.

In the second part of this thesis numerical simulations were performed to prove that bedrock meanders require sufficient alluvial cover and sediment supply for its formation and migration. Also, a numerical scale comparison of Kinoshita type meandering in alluvial and bedrock channels was performed.

<This dissertation is a modified and revised form of the following original journals and proceedings>

1. Jagriti Mishra, Takuya Inoue and Yasuyuki Shimizu,“ Simulations of Lateral Erosion in Bedrock Channels” 土木学会論文集 A2(応用力学), Vol. 72, No. 2 (応用力学論文集 Vol. 19), I_527-I_536, 2016.

2. Jagriti Mishra, Takuya Inoue and Yasuyuki Shimizu, “Comparision of Bedrock and Alluvial Meanders using 2 D Modelling” Journal of Japan Society of Civil Engineers, Ser. B1 (Hydraulic Engineering), Vol. 73, No. 4, I_835-I_840, 2017.

3. Jagriti Mishra, Takuya Inoue, Yasuyuki Shimizu, Tamaki Sumner and Jonathan Nelson, “*Consequences of Abrading Bed Load on Vertical and Lateral Erosion in a Curved Bedrock Channel”*, Journal of Geophysical Research- Earth Surface. (**Communicated**)

4. Mishra Jagriti, Kazutake Asahi, Yasuyuki Shimizu and Gary Parker, “*Numerical investigation of Channel evolution considering bank erosion and land accretion”*, 9th RCEM Symposium 2015, Iquitos, Peru.

5. Mishra Jagriti, Takuya Inoue and Yasuyuki Shimizu, “*Simulations of lateral erosion in bedrock channel”*, 19th Applied Mechanics Symposium 2016, Sapporo, Japan

6. Mishra Jagriti, Takuya Inoue and Yasuyuki Shimizu*, “Effect of bank erosion on bedrock sinuosity”*, 20th Congress of the Asia Pacific Division of the International Association for Hydro Environment Engineering & Research, IAHR APD 2016, Colombo, Sri Lanka

7. Jagriti Mishra, Takuya Inoue and Yasuyuki Shimizu, “*Comparision of Bedrock and Alluvial Meanders using 2 D Modelling”*, 61th Hydraulic Engineering Symposium, 2017, Kyushu, Japan.

8. Jagriti Mishra, Takuya Inoue and Yasuyuki Shimizu, “*A 2 Dimensional Study and Comparision of Migration and Skewness in Alluvial and Bedrock Meander”*, 10th RCEM Symposium 2017, Padova, Italy.

ACKNOWLEDGEMENTS

First and foremost, I would like to thank my supervisor Prof Yasuyuki Shimizu for accepting me as his student and the immense support and encouragement he has provided. His guidance helped me in all the time of research and writing of this thesis. He guided me not just in my studies but has also been a pillar of support who made my life easier and fun in Japan. He has been a teacher, a mentor, a friend, and a fatherly figure. I could not have imagined having a better advisor and mentor for my PhD study.

I would also like to take this opportunity to express my deepest gratitude towards Mr. Takuya Inoue. He has guided me through each small step towards achieving goals for this thesis. His motivation and patience with me, and the long ideas illuminating discussions have made this thesis possible.

I also owe a sincere gratitude to Prof. (Assoc.) Ichiro Kimura for his guidance, encouragement and appreciation for my work. All the stimulating discussions with him have contributed greatly to this thesis.

Also, I would like to thank Prof. Norihiro Izumi for his insightful suggestions. This thesis has greatly benefitted from his suggestions, criticisms and guidance.

I also thank Mr. Kazutake Asahi for his patience and support. He explained me his model a multiple times.

I thank all my fellow lab mates for warmly welcoming me in the lab and assisting me in many ways during these three years. In particular, I am grateful to Susumu Yamaguchi and Kazuaki Mutsuura for taking out time and helping me in experiments even on Sundays. I am also grateful to Ms. Tamaki Sumner and Mr. Daisuke Sato for their support and help during my experiments. I am grateful to Ms. Tamaki Sumner for the warm welcome and all the fun we have had in last three years.

Getting through my dissertation required more than academic support, and I have many people to thank for listening to and, at times, having to tolerate me over the past three years. I cannot begin to express my gratitude and appreciation for their friendship. In particular, I am grateful to Chetna Sharma, Maria Fernanda, Rahul Jog, Risa Suzuki Sasaki and Sayantani Chatterjee for being there in health and sickness and opening up their home and heart for me. I also owe a lot to all my long distant Indian friends for the long Skype sessions never letting me feel lonely. Taking out time and managing through so many different time zones indeed proves our love and dedication towards our friendship. I thank Nikhil Kumar for much-needed criticism, encouragement, humor and support.

Most importantly, I extend my special thanks to my parents and my sister for instilling confidence in me every time I doubted myself in my life. They enlightened me with the first glance of research. Nothing could have been possible without them. This dissertation stands as a testament to your unconditional love and encouragement.

Lastly, I want to thank all the taxpayers in Japan, MEXT and E^3, because of whom all the funding for this thesis work and also, my fellowship was possible.

TABLE OF CONTENTS

ABSTRACT.....i

ACKNOWLEDGEMENTS..... iii

TABLE OF CONTENTS.....iv

LIST OF FIGURES vii

LIST OF TABLES..... viii

Chapter -1 1

Introduction.....1

1.1. BACKGROUND AND MOTIVATION.....1

1.2 AIM, OBJECTIVES AND METHODOLOGY OF THE STUDY.....3

1.3 ORGANISATION OF THESIS.....3

Chapter -2 5

Vertical and Lateral Erosion in a U-Shaped Bedrock Bend Channel 5

2.1 INTRODUCTION 5

2.2 METHODS.....6

2.2.1 Particulars of Experimental Setup.....6

2.2.2 Measurement and Data Collection Techniques.....7

2.3 Experimental Conditions 8

2.3.1 *Experiment A:* Effect of varying sediment feed rate on bed and banks of bedrock channel8

2.3.2 Experiment B: Long-term evolution of bed and bank of bedrock channel when equilibrium sediment-supply condition is maintained.....8

2.4. Results.....15

2.4.1. Experiment A.....15

2.4.1.2 Bedrock Erosion.....15

2.4.2 Experiment B: Long-term evolution of bed and bank of bedrock channel when equilibrium sediment-supply condition is maintained. 21

2.5 Discussions 23

2.5.1 Bedrock erosion magnitude with increase in sediment supply 23

2.5.2 Relationship between lateral bedload transport and lateral bank erosion 24

2.5.3 Alluvial cover shape and bedrock bench formation....25
2.5.4 Implication for strath terrace and bedrock meanders....26
2.5.5 Equilibrium conditions for a longer duration of time....26
2.6 Conclusions....26
References....28
Chapter 3....32
Sine Generated Curve Laboratory Scale Experiments: Lateral and Vertical Erosion in alluvial covered Incised Meander....32
3.1 Introduction....32
3.2. METHODOLOGY....33
3.2.1 Particulars of experimental condition....33
3.2.2 Experimental data collection procedure....34
3.3. RESULTS AND DISCUSSION....34
3.4. CONCLUSIONS....36
REFERENCES....37
Chapter 4....38
Numerical Simulations to Imitate Lateral Erosion in Bedrock Channels....38
4.1 Introduction....38
4.2 Numerical Model....39
4.2.1 Flow model....39
4.2.2 Bed friction....40
4.2.3 Sediment transport and conservation....40
4.2.4 Bedrock bed erosion....41
4.2.5 Bedrock bank erosion....42
4.2.6 Effect of secondary flow....43
4.3 Calculation Condition....43
4.4 Simulations and discussion....44
4.4.1 Reproducing laboratory experiments.....44
4.4.2 Simulations to Identify Effect of Sediment Supply....45

4.5 Effect of Sediment Availability on Bedrock Channel....50
4.6 CONCLUSIONS....52
References....54
Chapter 5....56
Characteristic of Skewness in Meander Bends in Bedrock and Alluvial Channels....56
5.1. INTRODUCTION....56
5.2. NUMERICAL MODEL....57
5.2.1 Alluvial bank erosion....57
5.2.2 Land accretion....59
5.3. NUMERICAL CONDITIONS....59
5.4. RESULTS AND DISCUSSIONS....60
5.4.1 Comparing bedrock and alluvial meanders....60
5.4.2 Factors Affecting skewness in Bedrock Channel....61
5.4.2.1 Effect of Bed Angle....61
5.4.2.2 Effect of initial wavelength....63
5.5 CONCLUSIONS....64
REFERENCES....65
Chapter 6....66
Summary and Future Work....66
6.1 Summary and Conclusions....66
6.2 Future Work....67

LIST OF FIGURES

Figure 2.1 Images showing bends of Shimanto River…….. 6
Figure 2.2 Schematic diagram of flume……... 10
Figure 2.3 Data Collection points in the flume…… 11
Figure 2.4 Measurement Details…….. 11
Figure 2.5(a) Picture showing mould of flume (b) Arrow depicting the bedrock bed erosion depth in mould (c) Arrow depicting bedrock bank erosion in a mould… 12
Figure 2.6 Obtaining 3D scan of the mould……. 12
Figure 2.7 Snapshot of Experimental Flume…… 13
Figure 2.8 Snapshot of Experimental Flume…… 14
Figure 2.9 Bed Elevation shape along the centre of the channel……. 16
Figure 2.10 XYZ profile of 3D scan…… 19
Figure 2.11 Characteristics of maximum lateral and vertical erosion magnitude… 20
Figure 2.12 Characteristics of lateral erosion onset location……... 21
Figure 2.13 Snapshot taken after 16 hours of sediment equilibrium condition…... 22
Figure 2.14 Bed elevations along the centre of the channel after 4^{th} and 16^{th} hour of sediment supply condition……... 23
Figure 2.15 Graph showing increase in bank erosion with increase in lateral bed slope……. 25
Figure 3.1 Experimental flume of Sine Generated Curve Shape…… 33
Figure 3.2 (a) Mould of the fume (b) Picture of mould showing bank erosion in the flume marked with an arrow……... 35
Figure 4.1 Definition of L_{bank}…….. 41
Figure 4.2 Comparison of bank erosion width in simulation results with laboratory experiment results…… 43
Figure 4.3 Comparison of location of maximum bank erosion depth, measured from Upstream end…….. 44
Figure 4.4 Simulation results showing dimensionless areal fraction of alluvial cover……. 46
Figure 4.5 Effect of sediment feed rate in simulations…… 47
Figure 4.6 Effect of sediment feed rate. Comparison of point of maximum lateral erosion measured from bend apex in simulation results…….. 48
Figure 4.7 Bedload Flux in m^2/s…….. 49
Figure 4.8 Effect of sediment on bedrock channel…….. 51
Figure 5.1 Kinoshita type meandering in Atlanta river, Alaska…….. 56
Figure 5.2 Meandering Shikaribetsu river in Hokkaido…….. 56
Figure 5.3 Variables used in river bank erosion model……... 57
Figure 5.4 Meander bend migration……..... 60
Figure 5.5 Effect of bed angle on skewness of bedrock……..…… 62
Figure 5.6 Effect of initial wavelength on skewness of bedrock……. 63
Figure 5.7 New wave formation as wavelength increases……... 64

LIST OF TABLES

Table 2.1 Experimental Conditions…….. 9

Table 2.2 Measured data…….. 17

Table 2.3 Measurement taken after 16 hours of sediment equilibrium condition… 22

Table 3.1 Experimental Conditions…….. 34

Table 4.1 Calculation Conditions……. 43

Table 4.2 Sediment cover thickness……. 50

Table 5.1 Hydraulic Conditions……... 59

Table 5.2 Bed Angles for finding skewness of Bedrock channel…… 61

Table 5.3 Initial wavelength for finding natural wavelength and skewness of Bedrock channel……... 63

Chapter -1

Introduction

In this thesis, an attempt has been made to understand the process of erosion in Bedrock meanders. Several laboratory scale experiments were conducted to understand the process of erosion in bedrock channels. The focus was on erosion caused due to abrading bedload in a bend. The relationship between sediment flux and vertical and lateral erosion in bedrock bend was stablished post multiple laboratory scale experiments and on-field observations. These relationships were numerically implemented and tested to produce desirable results.

1.1. BACKGROUND AND MOTIVATION

As Japan is a geologically young country, the terrain reacts rapidly to mass movements by rain, snow, earthquake etc. Rivers are worst affected by these rapid changes, especially during large sediment discharge. Considering the planning of Japanese cities, it is essential and also prevalent in Japan to construct river embankments in order to straighten the river. Japan, being a country with higher rates of precipitation often suffers from mass sediment discharge during high rainfall seasons. Higher sediment discharge often leads to destruction of bank embankments, flooding of floodplain and in worse scenarios flooding of cities.

Almost all rivers tend to follow a sinusoidal shape as they move. This sinusoidal shape is determined by various factors, with the key factors being climate and discharge conditions, sediment load, local tectonics and rock strength of channel. It is vital to have tools that can predict the change in a river's path. Having understanding of factors effecting a river's migration will not only assist in protection and construction of civil projects but will also aid in understanding the evolution of earth planform.

Like alluvial rivers, Meandering is a phenomenon common in Bedrock Rivers also. A major number of studies conducted to understand meandering phenomena have concentrated their focus on alluvial meandering [Parker 1976, 2011 and Asahi 2013]. The characteristics of meandering in alluvial and bedrock channels are noticeably different from one another. To expand our understanding of landscape formation, it is vital that we understand bedrock channel characteristics as well as alluvial channel characteristics.

Bedrock channels are channels with very little or no alluvium; their bed and banks consist primarily of exposed bedrock. They are typically formed in situations in which

the supply of sediment to a channel is significantly less than the sediment transport capacity of that channel [Lawrence 2009]. The various factors contributing to the adjustment of landforms by bedrock channels can be broadly classified as follows: 1) Climate and discharge conditions [Stark 2006]: The mean discharge in a year and the number of flood witnessed guide the evolution and path of a river. 2) Substrate properties [Montgomery 2004]: The rock strength determines the ease and extent of bedrock surface erosion. 3) River sediment load [Hancock and Anderson 2002]: Sediment supply and grain size distribution can determine the erosion and hence the shape of bedrock channels. 4) Tectonic forcing [Harbour 1998]: An uplift or deformation in the land can force bedrock channels to change shape.

Although flow and bed evolution in alluvial meanders is well-studied and understood, this is not true for commonly observed bedrock meanders, where neither the mechanism of erosion nor observed morphology has received much attention. The inadequate efforts made to explore behaviour of bedrock meanders have confined our perception of landscape and topography. The morphology of a bedrock channel is determined by various factors like climate and discharge conditions, sediment load, local tectonics, and rock strength of the bedrock. In this study, I have made an attempt to explore the role that abrasion of bedrock by sediment particles moving as bed load will have in a curved bedrock channel. I conducted physical experiments to estimate the efficacy and spatial pattern of abrading sediment for eroding the bedrock bed and banks in a simple U-shaped channel bend with erodible bed and banks. In the experiments, the bed was initially covered with a thin layer of alluvial sediment in order to include the effect of protection of the bed by cover. Multiple experiments were conducted to observe the changes occurring in a bedrock bend associated with changes in sediment flux. The experiments showed that vertical incision had a more complex relation with the sediment feed rate, with an initial increase in abrasion as the feed rate increased followed by a decrease in abrasion of the bed as cover effects became important at higher feed rates. However, in the bend, lateral abrasion followed a monotonically increasing linear relationship with the sediment feed rate.

As meandering is a relatively slow phenomena (decades to centuries or more) not particularly conducive to experimental study, numerical tools have been invaluable for understanding their evolution. Most such land evolution models are based on the intuitive belief that an increase in fluid shear stress would result in increased bedrock incision [Stock and Montgomery 1999; Whipple and Tucker 1999, 2002; Whipple et al. 2000]. This assumption has been observed in field survey data as well [Howard and kerby 1983].

The saltation abrasion model took into account and tested the efficacy of abrading sediment particles to cause erosion of bedrock channel bed [Sklar and Dietrich 2001, 2004, 2006]. Notably, this approach bought into attention the contradicting effect sediment can have on the bedrock erosion- high sediment loads produce more saltating particles, but they also tend to produce coverage for the bedrock surface, thereby protecting that surface from abrasion. In the saltation abrasion models, these competing processes are called the *tools effect* and the *cover effect*, as named by its first observer [Gilbert 1877]. The tools effect causes increased abrasion in beds of bedrock with increased sediment flux, because the number of particles colliding with the bedrock

surface increases. On the other hand, the cover effect has a negative sediment flux dependency because higher sediment supply causes deposition of sediment in the beds potentially providing a cover against further abrasion by colliding particles [Gilbert 1877]. Efficacy of the tools and cover effect has been tested and found effective in various field studies [Johnson et al. 2010, 2009, Cowie et al. 2008]. Some numerical and laboratory studies have also confirmed the contradicting role sediment plays in determining shapes of bedrock channel [Finnegan et al., 2007; Inoue et al., 2014].

These limited attempts made to explore the formation mechanism of bedrock channels have restricted their attention to exploring the effect of vertical erosion in bedrock channels [Sklar and Dietrich 2001, 2004]. However, having knowledge regarding vertical abrasion alone is not sufficient for explaining the processes giving rise to bedrock meanders. To understand the evolution of bedrock meanders, the factors responsible for lateral erosion in bedrock must also be understood. The importance of lateral bedrock abrasion has been recognized in field observations [Seidl and Dietrich 1992, Cook et al 2014]. The formation of strath terraces provides clear evidence of what happens when lateral erosion dominates vertical erosion in bedrock channels [e.g., Fuller et al. 2009, Limiya and Lamb 2014, Inoue et al. 2017]. Some field studies conclude that a climate-driven increased sediment supply increases the abrasion of sediment to the banks of bedrock channels eventually increasing the lateral bedrock erosion [Stock et al., 2005].

1.2 AIM, OBJECTIVES AND METHODOLOGY OF THE STUDY

The aim of this study is to understand the process of meandering in both alluvial and bedrock meanders, with a primary focus on exploring bedrock meanders and the literature regarding the same is scarce. Following objectives were achieved in order to achieve the aim of this thesis:

1. Perform laboratory scale experiments to understand the factors effecting meandering process in bedrock channels.

2. Identify the dominating factor that controls the migration of a bedrock channel.

3. Establishing relationship between various factors and bedrock meander migration rate.

4. Numerical implementation of stablished factors and testing the numerical model for producing desirable results by exploiting it to reproduce various laboratory and on-field scale observations.

1.3 ORGANISATION OF THESIS

This thesis is drafted into 6 chapters, as following:

Chapter 1: This chapter includes the background work as well as the motivation behind

this thesis. It also explains the aims and objectives of this thesis.

Chapter 2: This chapter contains the detailed explanation regarding the laboratory scale experiments carried out in U- shaped bend bedrock channel. The chapter includes experimental conditions, methods and results of the U-shaped channel laboratory experiments.

Chapter 3: This chapter contains the background, experimental conditions, methods and results regarding the laboratory scale experiments carried out in Sine Generated Curves in order to get a clearer insight of effect of sediment on the curves of a bedrock channel.

Chapter 4: This chapter contains the introduction, a detailed explanation of the numerical model implemented to calculated bedrock studies, calculation conditions for the simulation and results obtained after numerical calculations. This chapter deals exclusively with numerical model and calculations performed for bedrock channel.

Chapter 5: This chapter includes brief explanation of the pre-implemented alluvial model exploited in this study in order to re-produce the on-field observed morphological differences between alluvial and bedrock meandering channels.

Chapter 6: This chapter summarises the findings of this thesis. Also, it includes suggestions for future work.

Chapter -2

Vertical and Lateral Erosion in a U-Shaped Bedrock Bend Channel

Although flow and bed evolution in alluvial meanders is well-studied and understood, this is not true for commonly observed bedrock meanders, where neither the mechanism of erosion nor observed morphology has received much attention. The inadequate efforts made to explore behavior of bedrock meanders have confined our perception of landscape and topography. The morphology of a bedrock channel is determined by various factors like climate and discharge conditions, sediment load, local tectonics, and rock strength of the bedrock. In this study, we have made an attempt to explore the role that abrasion of bedrock by sediment particles moving as bed load will have in a curved bedrock channel. We conducted physical experiments to estimate the efficacy and spatial pattern of abrading sediment for eroding the bedrock bed and banks in a simple U-shaped channel bend with erodible bed and banks. In the experiments, the bed was initially covered with a thin layer of alluvial sediment in order to include the effect of protection of the bed by cover. Multiple experiments were conducted to observe the changes occurring in a bedrock bend associated with changes in sediment flux. The experiments showed that vertical incision had a more complex relation with the sediment feed rate, with an initial increase in abrasion as the feed rate increased followed by a decrease in abrasion of the bed as cover effects became important at higher feed rates. However, in the bend, lateral abrasion followed a monotonically increasing linear relationship with the sediment feed rate.

2.1 INTRODUCTION

Previous laboratory-scale experiments intended to discover the relationship between erosion and bed load particle impact have enhanced our knowledge about the efficacy of bed load in straight channels [Fuller et al, 2016]. Their experimental results show that lateral erosion rate increases with increasing roughness of bedrock bed surface. Their findings create a new question for us. As sediment supply increases, the unevenness of bedrock surface is covered by sediment leading into a declination of bed roughness and lateral erosion rate. However, previous field survey suggests that strath terraces are easily formed when channel bed is almost covered by sediment [e.g., Stock et al. 2005, Fuller et al. 2009]. This implies the possibility that lateral erosion rate in the bend of a channel depends not only on roughness parameter but also other factors. In addition, a recent field visit to Shimanto River in Kochi prefecture of Japan (see Figure 2.1) served as a motivation to find out (1) why is bedrock bench formed near outer bank?; and (2) which part of bedrock bank is eroded with increasing sediment supply? In this study, the

intent is to generalize this understanding to the effect of bed load particle impacts in a curved bedrock channels, where both lateral and vertical erosion play important roles in the formation and evolution of the channel. This is the first time an attempt has been made to examine the effect of abrading sediment in a bedrock bend.

Figure 2.1: Images showing the bends of Shimanto River.

2.2 METHODS

2.2.1 Particulars of Experimental Setup

We conducted experiments using a U-shaped channel bend as shown in the **Figure 2.2(a)** and **Figure 2.2(b).** The experiments were conducted at Civil Engineering Research Institute for Cold Region (CERI), in Sapporo, Japan. The flume consisted of

soft mortar with erodible bed and banks. The flume was 3.88 meters in length with a width of 12cm. The height of flume was 10cm, and radius was 28cm **Figure 2.2(a)**. The scale of flume is taken roughly as 1/1000 of Shimanto River in Kochi, Japan. The Shimanto River is approximately 110m to 130m wide, with a curvature of approximately 260 m to 400 m, the approximate average width is 120 meters and curvature is 300 meters.

The flow discharge rate, initial bed slope, initial alluvial thickness, grain size were all kept constant throughout the experiments described here. We conducted four experiments with varying sediment feed rate in order to observe the effect of sediment supply on a curve in a bedrock channel. The bed load grain size was well sorted and kept constant with a diameter size of 0.0012 meters. The slope of channel was 0.0075 for all experiments with a water discharge of $0.001276 m^3/s$. At the upstream end of the flume, a soft mesh was kept in between water supply and upstream of the flume in order to make sure that water pressure did not cause erosion in the bed and banks at the upstream end of the flume. The sediment was fed manually at the upstream mouth of the flume. At the downstream end, all the sediment and water flowed into a sieve where sediment was collected. Downstream from the sieve, only water flowed to the flume tail tank and was eventually re-circulated to the upstream of the flume.

2.2.2 Measurement and Data Collection Techniques

During the experiments, water level and bed elevation were measured every 0.5 meters of the straight part of flume, using a point gauge. Water level and bed elevation for the straight part of the flume were measured only at the center of the channel. In the curved region of the flume, measurements were taken every 45˚ (starting from 0˚) at the near left bank, center and near right bank of the flume. The point of data collection at the near left bank was 3 cm from left bank, point of collection at the center is 6 cm from left bank and the point of data collection of right bank is 9 cm away from the left bank. **Figure 2.3** shows the data collection points for bed elevation and water level. The water level and bed elevation were measured every 1^{st}, 2^{nd} and 4^{th} hour of experiments. The sediment output rate was measured after every 30 minutes.

Once the experiments ended, the flume was left to dry for one day and then the sediment was removed from the flume using a vacuum cleaner. We added a straw at the mouth of the vacuum cleaner and then air was blown through the straw. Once all the sediments were removed, we prepared plaster of Paris and used it to create a mold of the flume. **Figure 2.5(a)** shows the mold created after experiment. The mold is a lateral and vertical inversion of the flume, i.e. the right bank of flume is left bank of the mold and left bank of flume is represented by right bank of the mold. Also, the bed shape of the flume is represented by the top layer face of the mold. The magnitude of lateral and vertical incision was obtained manually using a measuring tape. It was made certain that abrasion caused by bed load only was taken into account. In our experiment the sediment was bed load only, therefore only bedrock bank near the bed was eroded as shown in **Figure 2.3 (b)**. **Figure 2.4(a)** shows the definition of bedrock bank erosion start point and bedrock bed erosion (scouring) start point. Bedrock bank erosion start

point is the location at which bedrock bank started eroding due to collision with sediments. Bedrock bed erosion start point is the location at which bedrock was exposed and sediment could abrade the bedrock.

A 3 dimensional scan of the flume mold was taken using a DotProduct scanner (DotProduct scanner is a handheld tablet, android-based scanner, www.dotproduct3d.com). **Figure 2.6** was taken while scanning the mold. Pictures were taken at the 1st, 2nd and 4th hour of the experiment.

2.3 Experimental Conditions

2.3.1 *Experiment A:* Effect of varying sediment feed rate on bed and banks of bedrock channel

In this section, we conducted four experiments, numbered as Case 1, Case 2, Case 3, and Case 4. The sediment supply rate is 35ml/min in Case 1, 70ml/min in Case 2, 100ml/min in Case 3 and 140ml/min in Case 4. The sediment supply rate of 70ml/min is roughly equal to the sediment transport capacity for the straight part at initial condition (68ml/min).

The sediment-transport capacity for the straight part was calculated using the Meyer-Peter-Müller equation [Meyer-Peter-Müller,1948]

$$q_{bv} = 8\left(\tau_* - \tau_{*c}\right)^{1.5}\left(\sqrt{sgd^3}\right) \tag{2.1}$$

where q_{bv} is the sediment-transport capacity of straight channel, defined as the maximum amount of sediment that can flow through a channel under given hydraulic conditions maintaining a thin layer of bed alluvial deposition to provide cover effect, τ_* and τ_{*c} represent the dimensionless shear stress and dimensionless critical shear stress respectively, s is the specific gravity of submerged sediment taken as 1.65, g is the gravitational force taken as 9.8m/s, and d is sediment grain size. Dimensionless shear stress was calculated using the formula $\tau_* = hi/sd$. where h is water depth and i is the slope In fact, the alluvial bed elevation of straight parts did not change largely in Case 2.

All of these experiments were run for 4 hours. More detailed information regarding experimental conditions is mentioned in **Table 1.**

2.3.2 Experiment B: Long-term evolution of bed and bank of bedrock channel when equilibrium sediment-supply condition is maintained.

Our purpose for this experiment was to identify the consequence of supplying the equilibrium sediment flux over a longer time in a bedrock channel. Using a sediment of grain size 0.0012 metres, sediment feed rate of 70ml/min as in Case 1 was provided. All the hydraulic and physical conditions for this experiment were taken identical to Case 1 of Experiment A, except that this experiment was conducted for a much longer time. We continued running the experiment for 16 hours and allowed the topography to evolve.

Case	Slope i	Grain size diameter d (m)	Water depth h (m)	Velocity v (m)	Discharge q (m3/s)	Sediment feed rate (ml/min)
Case 1	0.0075	0.0012	0.02	0.532	0.001276	35
Case 2	0.0075	0.0012	0.02	0.532	0.001276	70
Case 3	0.0075	0.0012	0.02	0.532	0.001276	100
Case 4	0.0075	0.0012	0.02	0.532	0.001276	140

Table 2.1: Experimental Conditions

(a) Top view of the flume

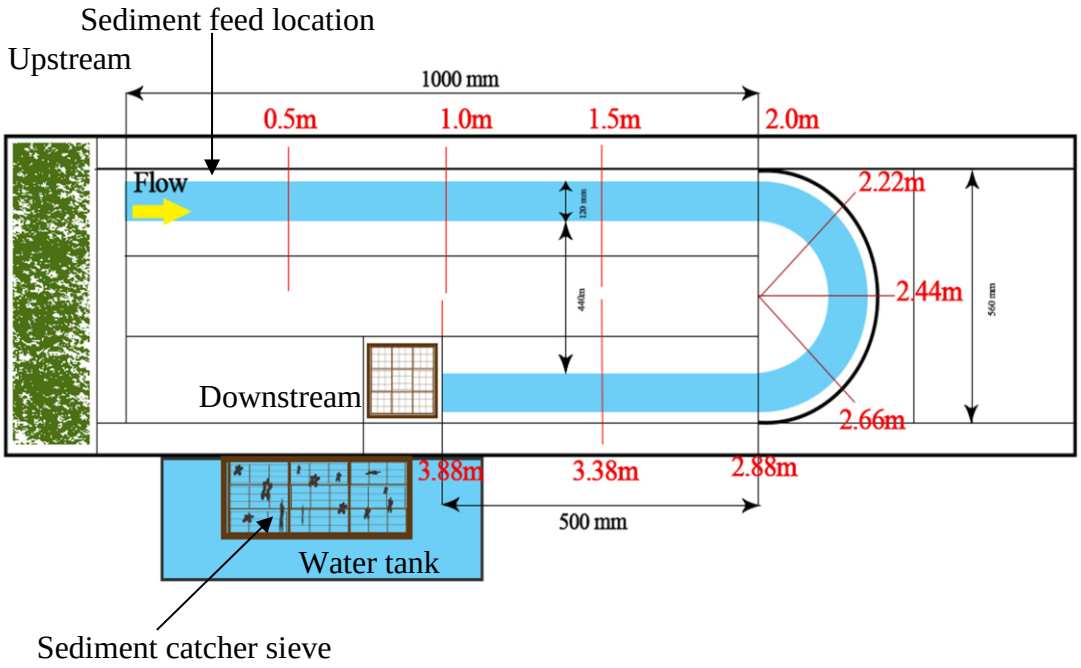

(b) Cross-sectional View of flume

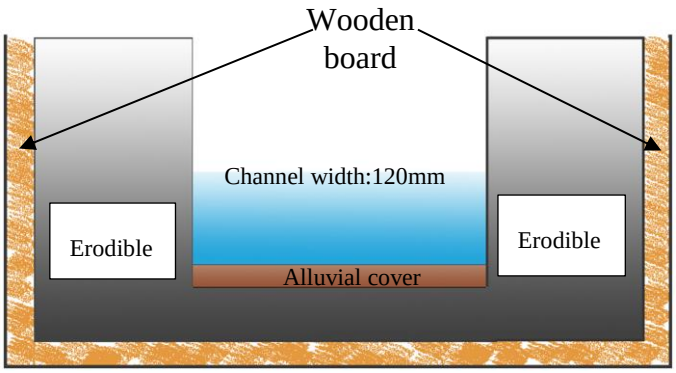

Figure 2.2: Schematic diagram of flume. a) Top view of the flume. Mesh was used near the mouth of the flume to make sure water pressure did not affect the alluvial bed or banks in the upstream. A sieve was kept in the downstream end to catch all the sediment so no sediment was recirculated with the water. . b) Cross-sectional view of the flume. Initial alluvial cover of 1.5mm thickness was maintained in the channel taking into account that most bedrock rivers are semi alluvial and have a thin alluvial cover.

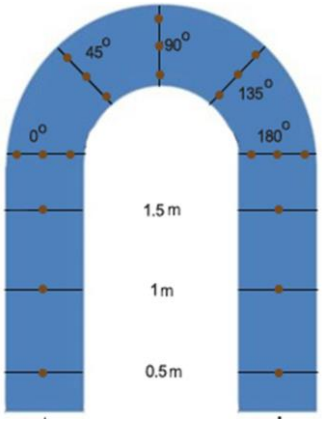

Figure 2.3 Data collection points in the flume.

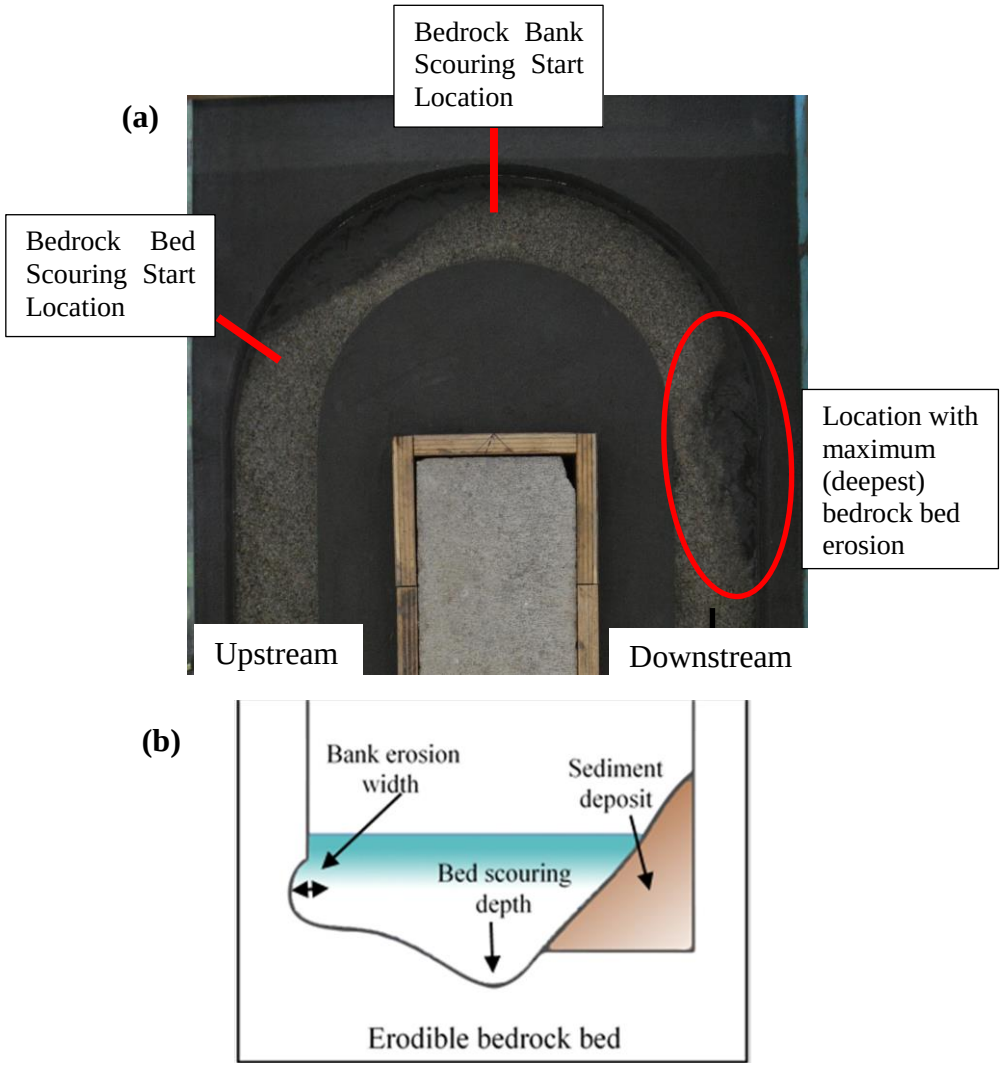

Figure 2.4: Measurement details. (a) Snapshot showing the start location of bedrock bed erosion and bedrock bank erosion. The location with deepest bedrock bed erosion is also highlighted. (b) Definition of bank and bed erosion, and bed elevation.

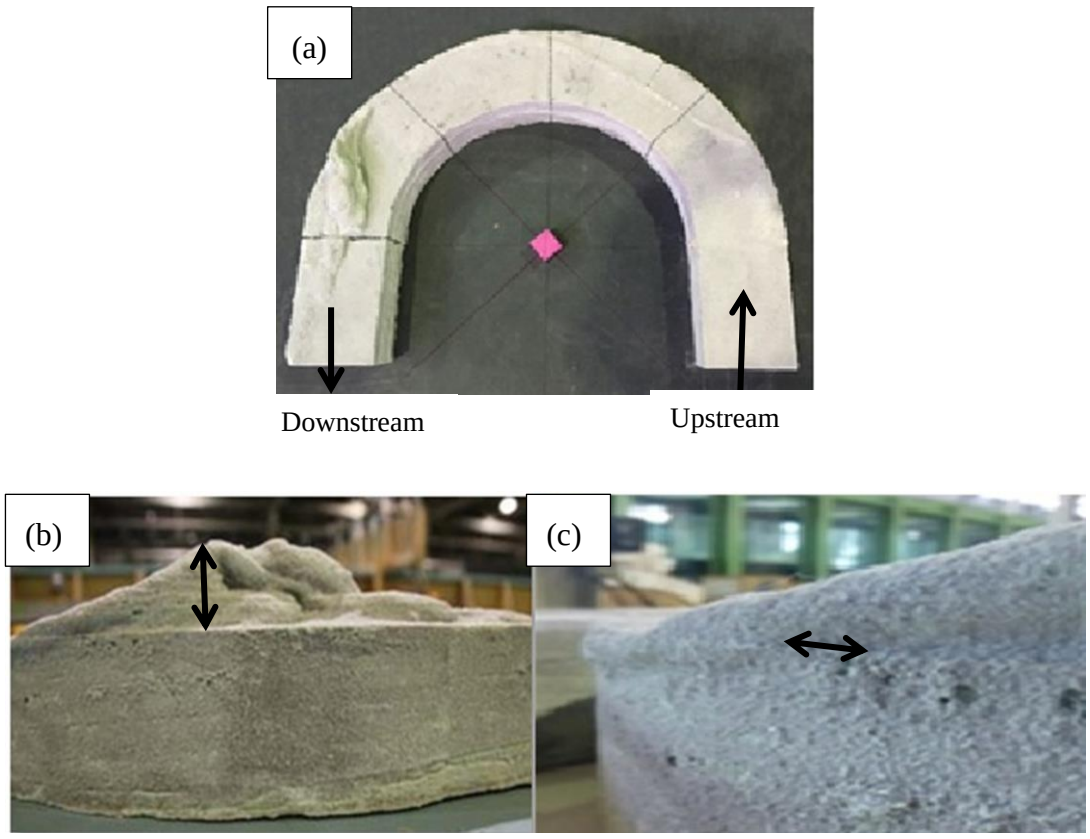

Figure 2.5 (a) Picture showing mold of the flume (b) Arrow depicting the bedrock bed erosion depth in a mold. (c) Arrow depicting bedrock bank erosion in a mold.

Figure 2.6 Obtaining 3D scan of the mold

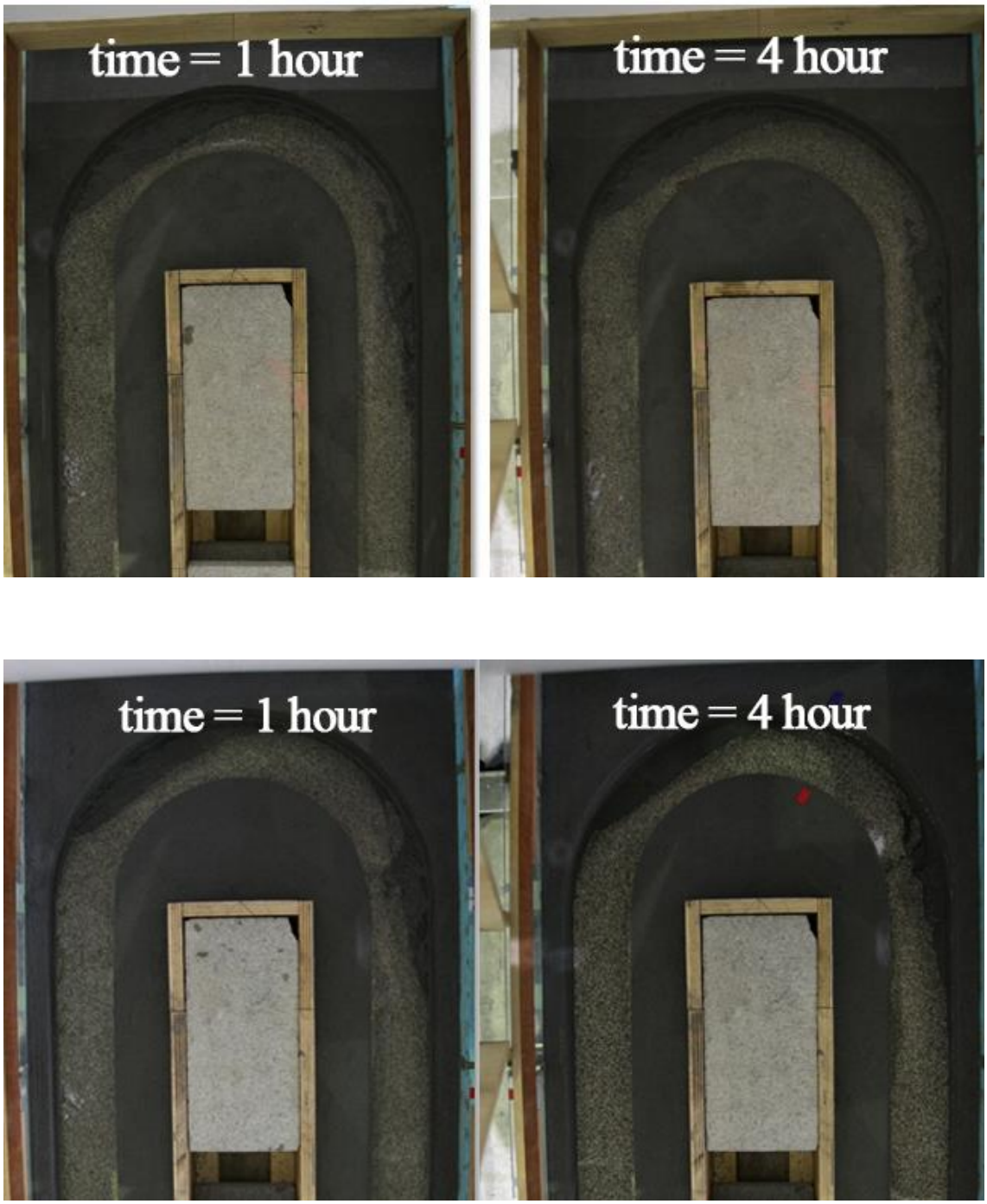

Figure 2.7: Snapshot of experimental flume at time = 1 hour and time = 4 hour. (a) Snapshots for Case 0.5. (b) Snapshots of Case 1. At time=4 hours of (a) and (b), it is apparent that bedrock in (a) is more exposed as compared to bedrock in (b).

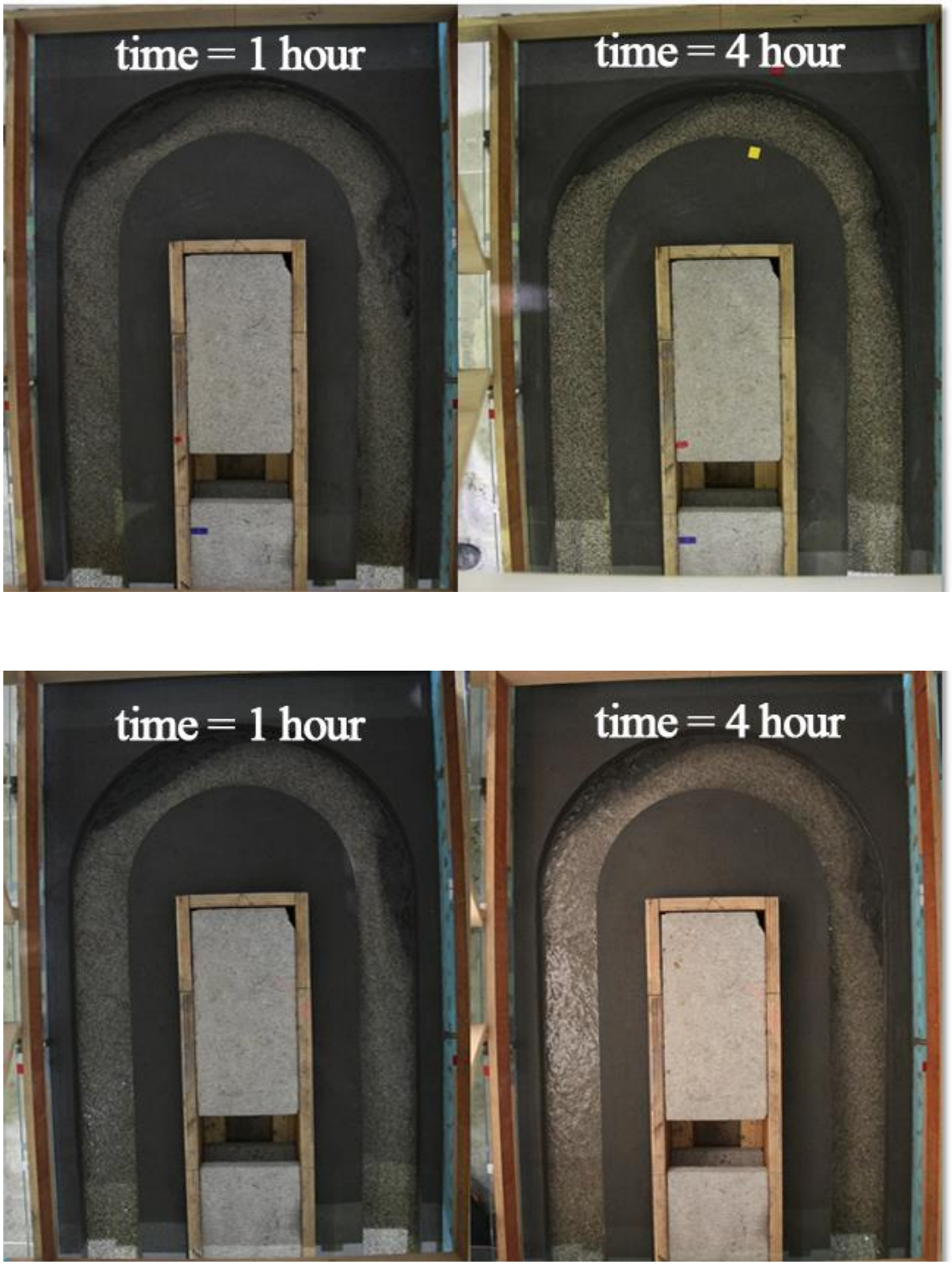

Figure 2.8: Snapshot of experimental flume at time = 1 hour and time = 4 hour. (a) Snapshots for Case 1.4. (b) Snapshots of Case 2.

2.4. Results

2.4.1. Experiment A

2.4.1.1 Alluvial Cover Shape

Figure 2.7 and **Figure 2.8** provide photographs of the flume taken during the experiment. The dark grey part represents the flume and exposed bedrock. The light brown color represents the sediment cover. **Figure 2.7** shows the shape of sediment cover in case 1 from 1st hour to 4th hour. The outer bank towards the upstream of the bend apex has an exposed bedrock bed. An exposed bed can also be noticed towards the downstream of the bend. A similar tendency can be observed in all the cases.

In Case 2, a sediment flux of 70ml/min was supplied throughout the experiment. In the first hour of the experiment, sediment outlet rate observed at downstream end of the flume was not equal to the sediment supply rate. An output of 70ml/min was achieved after first hour of the experiment. Before 1st hour, the sediment mainly got deposited in the inner bend and formed a point bar. **Figure 2.9** shows the bed elevation along center line from 0 hour to 4th hour of experiment. We observed that the bed elevation of straight part did not change largely. This indicates that sediment supply rate is roughly equal to the sediment transport capacity in the straight part.

When we reduced the sediment feed rate to 0.5 times of Case 2, i.e. 35ml/min for Case 1, bedrock exposed area in the vicinity of the concave part of channel increased from Case 2 (shown in **Figure 2.7**).The ratio of sediment output to sediment input , as observed after 4th hour of experiment was 0.9371.
We then increased the sediment input to 1.4 times of Case 1. A sediment feed rate of 100ml/min was taken in Case 3. In this case, the bed elevation of straight part increased. The bed elevation also increased in bend part. The rate of output/input at 4th hour is 0.97. Bedrock exposed area at upstream of bend apex is smaller than that in Case 2 (shown in Figure 2.8).

We further increased the sediment input to 2 times of equilibrium condition of Case 1. We fed sediment at the rate of 140ml/min in Case 4. In this situation we observed that sediment deposition occurred near the upstream end of the flume, increasing the bed elevation (**Figure 2.9**).

2.4.1.2 Bedrock Erosion

The lateral abrasion was confined to the bank surface near the bed, as the sediment used in this experiment was bed load only. As sediment moved as bed load, the effect of suspended sediment was not present.

In order to examine how the sediment feed rate governs the topography; we compared the results of all four cases. **Figure 2.10** provides the data obtained from 3D

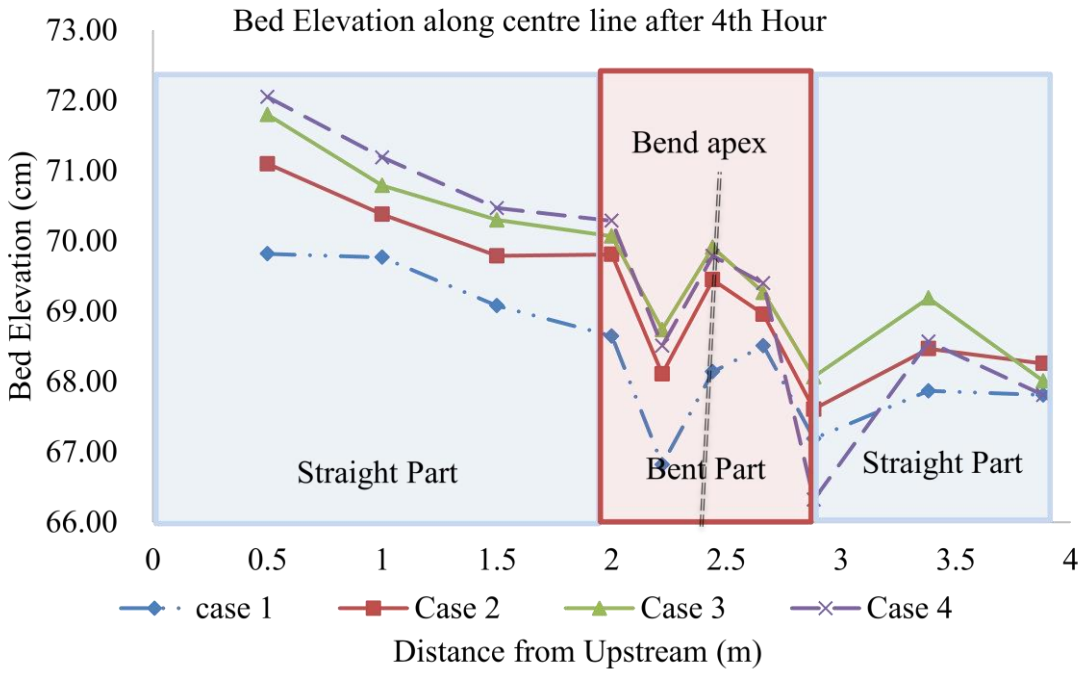

Figure 2.9: Bed elevation shape along the center of the channel

scan. **Figure 2.10(a)** represents the XYZ data obtained from 3D scan shows that channel near the upstream mouth (i.e. the upstream region of the bend) suffered from bed erosion. From 0 to 90 degrees in the bend, it can be seen that vertical abrasion due to saltating bed load particles started, with the magnitude of vertical abrasion increased near the curve, especially downstream of the bend apex. This vertical erosion occurred along the boundary of sediment cover. Downstream of the bend apex (from 112.5 degrees) lateral erosion can be observed. **Figure 2.10(b)** provides a guide to the degrees in the mold. **Figure 2.2(a)** shows the top view of the flume, as well as the distance of various points from upstream.

We also compared the 3D Scan of the bent part with the straight part of the channel. The straight part was completely covered with sediment during experiment (**Figure 2.10(c)**). The straight part of the channel shows no wall or bed erosion. We observed qualitatively that the sediment flowed parallel to the sidewall of straight section.

Due to the sediment deposition in the inner bend and an exposed outer bend, the bed near the outer bend became vulnerable to erosion caused by the abrading sediments. In Case 2, when the sediment is supplied in capacity condition, the bed was scoured intensively in the downstream region of the channel bend (Figure 2.10(a) 157.5 degree). The vertical abrasion of this zone had a small meander like shape, with an overhang occurring on the inner side. The maximum vertical erosion was observed in this zone, and the erosion depth was 43.4mm [**Table 2**]. The vertical erosion started at 14cm away from upstream. The bed abrasion start point or vertical erosion start is the location at which erosion of bed starts, demonstrated clearly in **Figure.2.4.** The lateral abrasion was also observed in the downstream region of the bend apex, starting at 59.2 cm away from Upstream of the channel. The measured maximum lateral abrasion rate after 4

hours of experiment was 3.5mm/4 hours.

In Case 1, as compared to Case 2, the maximum vertical erosion depth decreases at 32.5mm (**Table 2**). The location of maximum erosion point also is in the downstream region of the channel bend (**Figure 2.10a** 157.5 degree). The location of the vertical erosion point was shifted towards the upstream at 12.5cm, whereas lateral abrasion was shifted farther downstream at 78.3cm. In this case, negligible maximum lateral erosion occurred, the maximum being equal to 1mm/4hour.

In Case 3 as well, the maximum vertical erosion decreased to 33.5mm, as compared to Case 2.The starting point of vertical erosion was 17cm away from the Upstream of the channel. The maximum vertical erosion depth was 33.5mm. The lateral erosion in this case shifted towards the Upstream at 56.2cm with a magnitude of 7.5mm/4hour [**Table 2**].

In Case 4, when the sediment input was increased to 2 times of Case2, the maximum vertical erosion decreased to 29mm. The vertical erosion starting point was 16.5 cm away from Upstream of the channel. The lateral erosion start point shifted closer to Upstream, at 52.7cm from Upstream of the channel. The rate of lateral erosion was 12mm/4hour [**Table 2**].

Figure 2.11 shows the behavior maximum lateral and vertical erosion follows with respect to an increase or decrease in bed load. It was found that lateral abrasion increased linearly with increase in sediment feed rate, shown distinctly in **Figure 2.11 (a)**. On the contrary, it is evident from **Figure 2.11(b)** that vertical abrasion did not

Cases	Sediment feed rate (ml/5min)	Maximum Bank erosion width (mm)	Maximum bed erosion depth (cm)	Start point of bed erosion (cm)	Start point of bank erosion (cm)
Case 1	175	1	3.25	12.5	78.3
Case 2	350	3.5	4.34	14	59.2
Case 3	500	7.5	3.35	17	56.2
Case 4	700	12	2.9	16.5	52.7

Table 2.2: Measured data. The upstream initiation point of bed and bank erosion in this table is mentioned as measured from 0˚ upstream. The initiation point of bed and bank erosion is the location from which erosion started occurring. In the straight section of the upstream, no bank or bed erosion was observed.

share a linear relationship with sediment feed rate. Increasing the sediment feed rate initially increased the depth of bed abrasion and then showed a decline in magnitude of bed abrasion. The bed abrasion depth increased up to the sediment capacity condition, it thereafter started showing a decline.

Figure 2.12 reveals this relationship between sediment feed rate and the point in the channel where bed load starts abrading the bank. It affirms that lateral abrasion start location shifts upstream as bed load increases. It also indicates the relationship between increasing sediment supply with the farthest reach of bank abrasion. Bank abrasion end point shifts towards the downstream or shifts farther from upstream when sediment supply increases. Bank abrasion end point is defined as the farthest point in the channel until where sediment could abrade the wall, i.e. this is the farthest point sediment did not start flowing parallel to the walls.

In **Figure 2.9**, we can see the relationship between lateral bed slope and bank erosion magnitude. Bank erosion increases with increase in sediment supply as effect of lateral bed slope starts dominating effect of secondary flow, moving more and more sediment towards the outer bend.

The bank of channel witnessed erosion only due to abrasion which can happen only when sediment moves near the bank. Alluvial cover provides a proof for path of sediment flow. The places where bed is exposed or there is no sediment cover means no sediment flowed near the walls of the channel.

When we compared the straight part of the channel with the bent part, no lateral erosion has happened in the straight part of the channel. Although, the sediment flows near the wall in straight part, it causes no erosion as it flows parallel to the wall. This indicates that vector of sediment transport is important for lateral erosion.

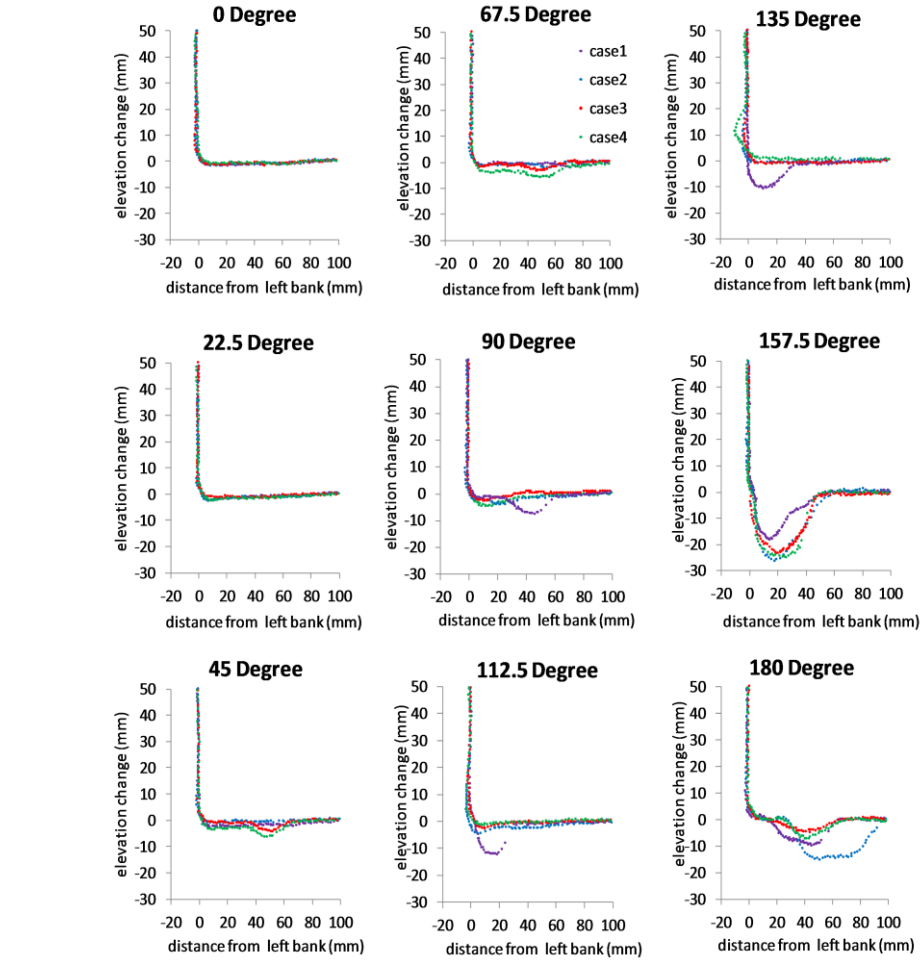

(b)

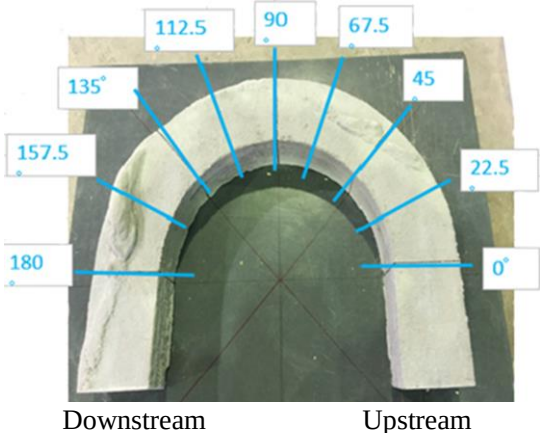

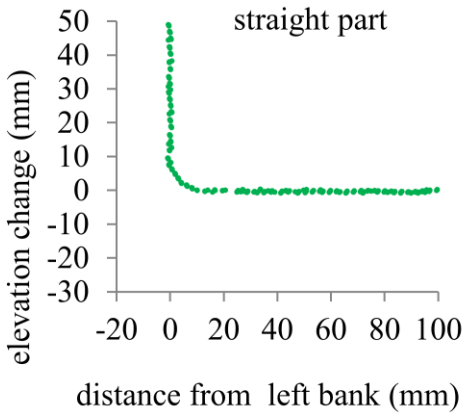

Figure 2.10: XYZ profile. (a) XYZ profile showing that bed scouring starts early, i.e. in the upstream of bend apex whereas bank erosion occurs towards the downstream of bend apex. (b) Various angles at which the XYZ profile was calculated are marked on the flume. (c) 3D scan of straight part shows no bed or wall erosion.

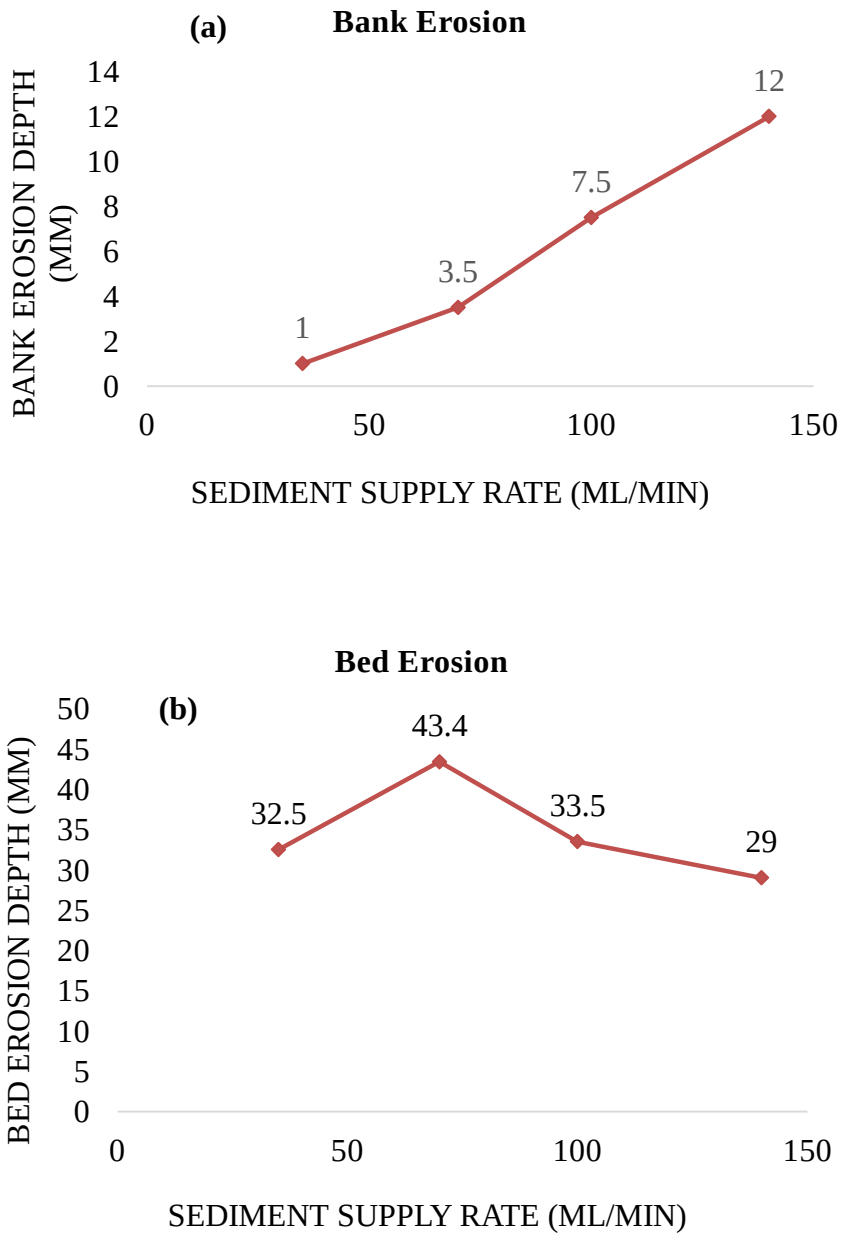

Figure 2.11: Characteristics of maximum lateral and vertical erosion magnitude. (a) Bank erosion magnitude with respect to bed load. Bank erosion followed a linear relationship with increase in sediment feed. (b) Bed erosion magnitude with respect to bed load. Bed erosion followed a non-linear relationship with increase in sediment feed rate. It initially increased with increase in sediment feed, after the equilibrium sediment condition, it started showing a decrease in magnitude.

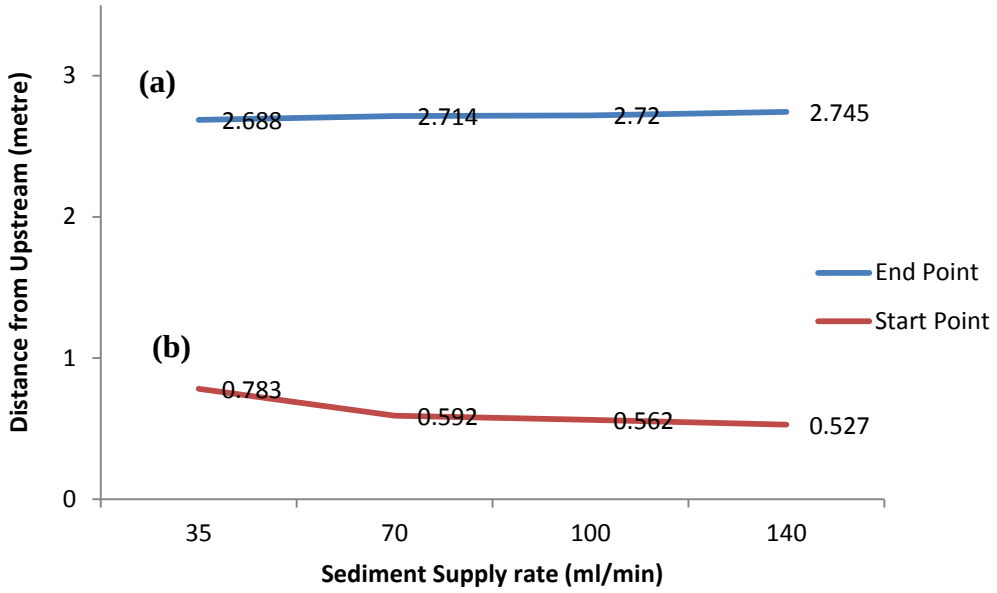

Figure 2.12: Characteristic of lateral erosion onset location. Sediment feed rate increases from Case 1 to Case 4. All the distances are measured in metres from the upstream mouth of channel. (a) Bank erosion initiation point or start point with respect to bed load. Bank or lateral erosion showed a decrease in distance from upstream, i.e. it moved closer to upstream with increase in bed load. (b) Bank erosion end point. The end point of bank erosion shifts away from upstream with increase in sediment feed.

2.4.2 Experiment B: Long-term evolution of bed and bank of bedrock channel when equilibrium sediment-supply condition is maintained.

Our purpose for this experiment was to identify the consequence of supplying the equilibrium sediment flux over a longer time in a bedrock channel. Using sediment of grain size 0.0012 metres, sediment feed rate of 70ml/min as in Case 1 was provided. All the hydraulic and physical conditions for this experiment were taken identical to Case 1 of Experiment A, except that this experiment was conducted for a much longer time. We continued running the experiment for 16 hours and allowed the topography to evolve.

Sediment feed rate	Maximum bank erosion width(mm)	Maximum bed erosion depth(cm)	Start point of bed erosion (cm)
350ml/5min	7	4.6	12.5

Table 2.3: Measurements taken after 16 hours of sediment equilibrium condition

Figure 2.13: Snapshot taken after 16 hours of sediment equilibrium condition.

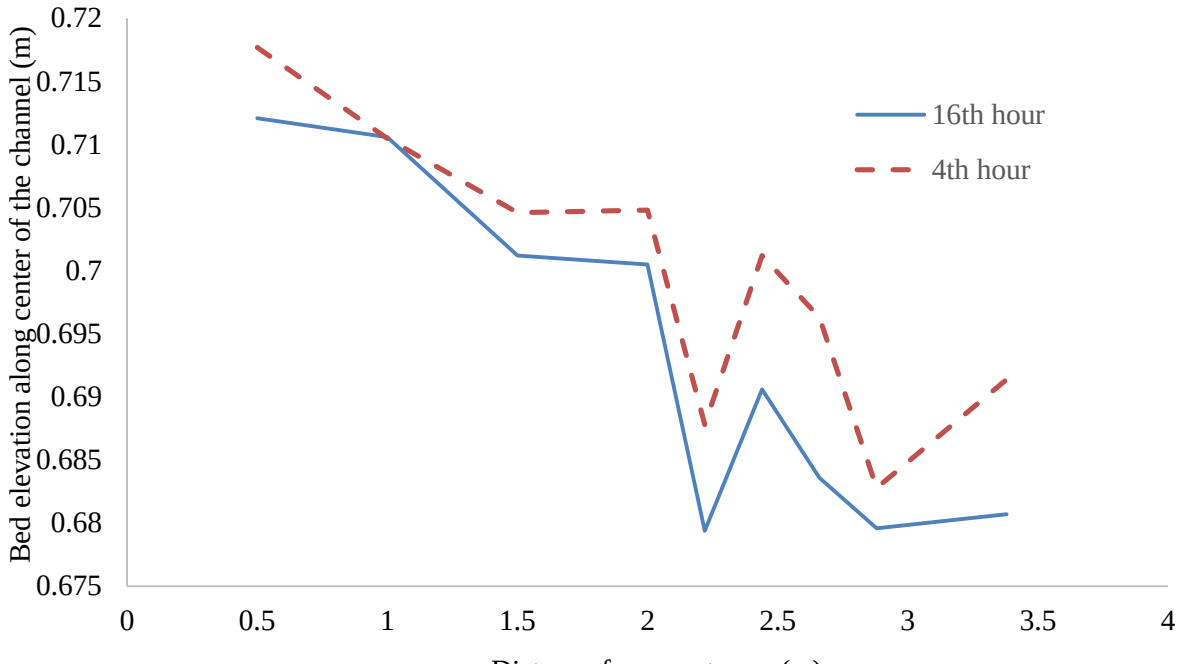

Figure 2.14: Bed elevation along the center of the channel after 4th and 16th hour of equilibrium sediment supply condition. The dotted line represents the bed elevation after 4th hour (Experiment A, Case1). The thick line is the bed elevation after 16 hours (Experiment B)

2.5 Discussions

2.5.1 Bedrock erosion magnitude with increase in sediment supply

Taking into account the findings of this study, we found that lateral abrasion increased linearly with increase in sediment flux, though it was confined near the bed surface, and that the magnitude of bed abrasion increased initially with increased sediment supply but subsequently declined as supply increased further. Bed erosion follows a nonlinear relationship with increase in bed load as the cover effect comes into play [Gilbert 1877, Sklar and Dietrich, 2001]. With the initial increase in bed load, the tools effect is more dominant, as a greater number of bed load particles collide with the bed and cause erosion. The bed abrasion showed a decline after the equilibrium sediment supply condition exceeded, above which the cover effect becomes dominant as more sediment gets deposited in the channel, eventually inhibiting the bed load from colliding with the bed and hence reducing the bed abrasion. Similarly, lateral erosion was found to be following a linear relationship with bed load, as no cover effect comes into play in the case of steep outer banks.

2.5.2 Relationship between lateral bedload transport and lateral bank erosion

The 3D scan comparison of the bent and straight part shows that bank erosion only occurred near the bent part of the channel. The straight part of the channel did not suffer any lateral erosion even though the sediment flowed near the walls. This happens because vector of bedload particles is important to erode the walls. Some laboratory experiments conducted in previous studies [Fuller et al., 2016] imply the role of varying bed roughness as a factor of controlling lateral erosion. The experiments in previous study were conducted in a straight channel and bed roughness varied along the length of the channel by introducing sediment of various sizes in cement bed as roughness element. The varied bed roughness caused the bedload particles to move towards the walls and abrade the wall. In our study, we have made an attempt to know the effect of sediment in a bent in the bedrock river. Meanders and bents are natural, inevitable phenomena in any natural water channel. In our study, we establish the relationship between sediment supply and a bent in channel. We are also able to prove that, vector of bedload is crucial to erode the walls of channel; given a condition of constant bed roughness, the sediment will flow parallel to the sidewalls of channel unless a change in shape of channel (bend, pit, etc.) changes the vector of the sediment and forces sediment towards the wall.

A widely used equation manifests the fact that lateral bedload transport rate is determined by the balance between the effect of lateral bed slope and the effect of secondary flow [e.g., Hasegawa, 1981; Mosselman and Crosato, 1991]. Secondary flow grows near the bends of channel, pushing the fluid in the center of the bend to move towards the outer bend and the fluid near the walls of the channel move inwards through near the river bed. This lateral flow causes bedload to move to inner bank. On the other hand, lateral bed slope rolls gravels to outer bank (Figure 2.15). With increased sediment input, the height of point bar increases, the effect of lateral bed slope dominates over effect of secondary flow making more and more sediment collide with the walls of the bank, causing more and more erosion to the banks. Previous studies have confirmed the effect of lateral sediment transport to maintain channel dynamics [Davy and Lague, 2009]. Lateral sediment transport is essential as absence of lateral sediment transport makes the channel deep, narrow and immobile [Schuurman et al., 2013].

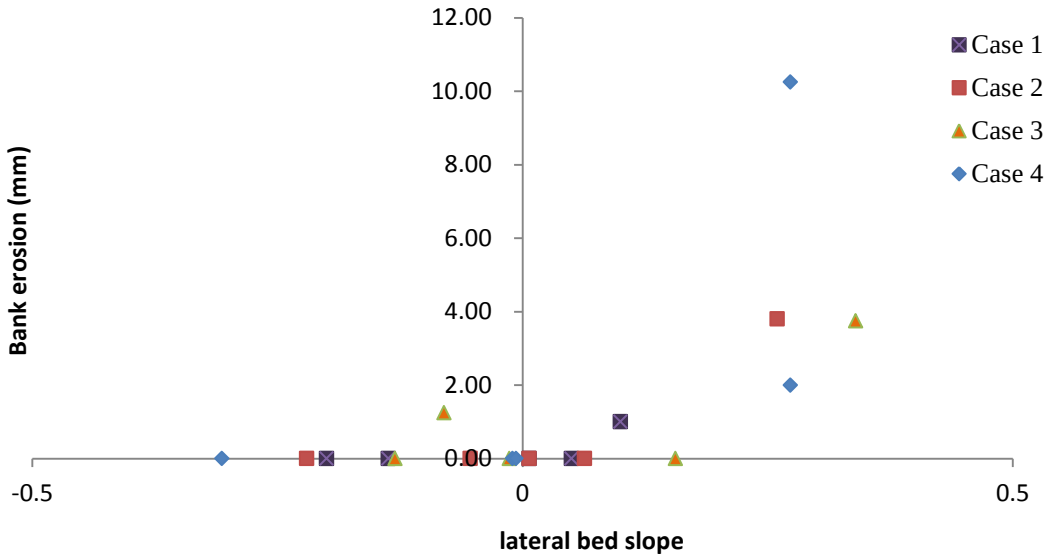

Figure 2.15. Graph showing increase in bank erosion with increase in lateral bed slope.

2.5.3 Alluvial cover shape and bedrock bench formation

Nelson et al. [2014] and Inoue et al. [2016] calculated shape and thickness of alluvial cover in a bend in a mixed bedrock-alluvial river. They showed that height and width of point bar increase with increasing sediment supply. Although this tendency is similar to our experimental result, planar shape of point bar is different from the calculated results of Inoue et al. [2016]. Because Inoue et al. [2016] used a spiral and uniform bend channel, the shape of point bar did not change along streamwise direction. In our experimental results, the width of point bar is not symmetric to the bend apex. Such asymmetric point bar is experimentally observed in a bend in an alluvial channel [Zolezzi et al., 2005; Blanchaert, 2010]. In case of narrow channels with sharp bends, the bed is symmetrical till the inflection points. An eroded and deep outer bank with deposition in the inner bend is observed immediately downstream to the inflection points [Zolezzi et al., 2005]. The width of channel plays a crucial role in defining the shape of bed, especially near the curves.

The flume experiments also suggest that bedrock erosion in case of bedrock rivers dominantly occurs in the center of the channel (at 0 degree to 90 degree) which is in contradiction to alluvial rivers in which the outer bend of the channel is scoured. Many previous studies conducted on alluvial channels prove that the shape of bed elevation in alluvial channels is deeper near the outer bend and shallow near the inner bend [e.g, Zolezzi et al., 2005; Blanchaert, 2010]. Bedrock erosion in the central part is influenced by the bedrock near the outer bank which is fully exposed with no sediment transport over it leading to a bedrock bench. The bedrock near the inner bank is completely covered by sediment with no erosion. As a result, the central part is eroded. A recent numerical study conducted over mixed bedrock-alluvial meander bend found the location of vertical incision was maximum inward from the outer bank in situations

where the alluvial point bar becomes narrower than the channel [Inoue et al., 2016]. Our experimental results prove that their simulation result is correct.

2.5.4 Implication for strath terrace and bedrock meanders

Some studies have credited the seasonal higher sediment supplies to be the driving force for lateral erosion and strath terrace formation [Gilbert, 1887; Molnar et al., 1994; Hancock and Anderson, 2002; De Vechhio et al., 2012]. Where a climate driven increase in sediment drives lateral erosion making it dominant over bed erosion [De Vechhio et al., 2012]. Our experimental results showed similar characteristic; although erosion in the vertical direction decreases when the sediment supply increases too much, erosion in the lateral direction linearly increases with sediment supply. Also, bedrock meanders with alluvial cover and nominal vertical erosion, have outer bank suffering lateral erosion. This leads into an alluvium covered bedrock river which later forms strath terraces given a possibility of vertical erosion [Finnegan and Dietrich, 2011; Limaye and Lamb, 2016; Finnegan et al.,2014]. This means that the direction of lateral erosion in bedrock meanders is important to predict the planer shape of terraces. Our observations showed that the bank downstream of bend apex is eroded and the area on the sidewall of the channel that comes in contact with sediment and gets abraded increases with increased sediment supply, i.e. when sediment availability increases, the length of lateral abrasion increases.

2.5.5 Equilibrium conditions for a longer duration of time

In this experiment, we intended to observe the way topography will be effected if equilibrium sediment conditions are maintained for long durations. The equilibrium condition was checked every hour by measuring the sediment output. Sediment output was measured by collecting the sediment at the downstream end in a sieve for 5 minutes and then measuring it manually using a flask. Figure 2.15 showcases the snapshots taken during Experiment B. When equilibrium conditions were maintained for a long period, we observed that the experiment followed similar behavior as Case 1 of Experiment A. The start point of bed scouring shifted towards upstream by 2.5 cm. Also, the maximum bed scouring depth increased by 0.26cm. The maximum lateral abrasion width of bank erosion showed an increase of 2 times, from being 3.5mm in Case 1 of Experiment A to 7mm in Experiment B. The measurements taken after Experiment B are mentioned in **Table 2.3**.

Figure 2.14 displays the bed elevation measured using a point gauge after the 4^{th} hour of Case 1 of Experiment A and 16^{th} hour of Experiment B. Bed erosion depth did not show a significant increase even after 16 hours of equilibrium condition.

2.6 Conclusions

The present study suggests that bed load is a powerful tool causing bed and bank

abrasion. An increase in sediment supply causes following: accelerates bank erosion by inhibiting bed erosion, an increase in area of bank erosion, Shifts start point of bank erosion towards the upstream, increases the length as well as the depth of bank erosion in bedrock channels. Also, the start point of bank erosion shift towards the upstream with increased time of exposure of banks to the sediment. Also, an increase in sediment supply makes the effect of lateral bed slope dominate over the effect of secondary flow. The present study also suggested that the bedrock channel bed is eroded in the center of the channel, contradicting the behavior of bed erosion in alluvial rivers that is dominant near the outer bend of the channel.

Our findings clarify the role of bed load in causing bed and bank abrasion and suggest that behavior of curved bedrock channels is critically dependent on the differences between lateral and vertical abrasion. These observations can contribute towards development and testing of stronger numerical tools.

References

1) Blanckaert, K. (2010). Topographic steering, flow recirculation, velocity redistribution, and bed topography in sharp meander bends. *Water Resources Research, 46*(9), n/a-n/a. doi:10.1029/2009wr008303

2) Cook, K. L., Turowski, J. M., & Hovius, N. (2014). River gorge eradication by downstream sweep erosion. *Nature Geoscience, 7*(9), 682-686. doi:10.1038/ngeo2224

3) Cowie, P. A., Whittaker, A. C., Attal, M., Roberts, G., Tucker, G. E., & Ganas, A, (2008). New constraints on sediment-flux–dependent river incision: Implications for extracting tectonic signals from river profiles. *Geology, 36*(7), 535. doi:10.1130/g24681a.1

4) Davy, P., and D. Lague (2009), Fluvial erosion/transport equation of landscape evolution models revisited, *J. Geophys. Res., 114*, F03007, doi:10.1029/2008JF001146.

5) DeVecchio, D. E., R. V. Heermance, M. Fuchs, and L. A. Owen (2012), Climate controlled landscape evolution in the Western Transverse Ranges, California: Insights from Quaternary geochronology of the Saugus Formation and strath terrace flights, Lithosphere, 4[2], 110-130, doi:10.1130/L176.1.

6) Finnegan, N J., Schumer, Rina; Finnegan, Seth (2014), A signature of transience in bedrock river incision rates over timescales of 104-107 years, Nature, Volume 505, Isuue 7483, pp. 391-394.

7) Finnegan, N. J., & Dietrich, W. E. (2011). Episodic bedrock strath terrace formation due to meander migration and cutoff. *Geology, 39*(2), 143-146. doi:10.1130/g31716.1

8) Finnegan, N. J., Sklar, L. S., & Fuller, T. K. (2007). Interplay of sediment supply, river incision, and channel morphology revealed by the transient evolution of an experimental bedrock channel. *Journal of Geophysical Research, 112*(F3). doi:10.1029/2006jf000569.

9) Fuller, T. K., K. B. Gran, L. S. Sklar, and C. Paola (2016), Lateral erosion in an experimental bedrock channel: The influence of bed roughness on erosion by bed load impacts, J. Geophys. Res. Earth Surf.,121, 1084–1105, doi:10.1002/2015JF003728.

10) Fuller T. K, Perg L. A, Willenbring J. K, Lepper K. (2009), Field evidence for climate-driven changes in sediment supply leading to strath terrace formation. Geology 37[5]: 467-470. doi:10.1130/G25487A.1 ER.

11) Gilbert, G. K. (1877), Report on the Geology of the Henry Mountains: Geographical and Geological Survey of the Rocky Mountain Region, 160 pp., U.S. Gov. Print. Off., Washington, D.C

12) Hancock, G., and Anderson R. S. (2002), Numerical modeling of fluvial strath terrace formation in response to oscillating climate, Geol. Soc. Am. Bull., Vol. 114, pp. 1131– 1142.

13) Hasegawa, K. (1981), Bank erosion discharge based on a non-equilibrium theory. *Proceedings of the JSCE*, Tokyo, 316, 37–50.

14) Howard, A. D., and G. Kerby (1983), Channel changes in Badlands, Geol. Soc. Am. Bull., 94[6], 739–752, doi:10.1130/00167606[1983]94<739:CCIB>2.0.CO;2.

15) Inoue, T., Parker, G., & Stark, C. P. (2017). Morphodynamics of a bedrock-alluvial meander bend that incises as it migrates outward: approximate solution of permanent form. *Earth Surface Processes and Landforms*. doi:10.1002/esp.4094

16) Inoue, T., Izumi, N., Shimizu, Y., & Parker, G. (2014). Interaction among alluvial cover, bed roughness, and incision rate in purely bedrock and alluvial-bedrock channel. *Journal of Geophysical Research: Earth Surface, 119*(10), 2123-2146. doi:10.1002/2014jf003133.

17) Johnson, J. P. L., Whipple, K. X., & Sklar, L. S. (2010), Contrasting bedrock incision rates from snowmelt and flash floods in the Henry Mountains, Utah. *Geological Society of America Bulletin, 122*(9-10), 1600-1615. doi:10.1130/b30126.1

18) Johnson, J. P. L., Whipple, K. X., Sklar, L. S., & Hanks, T. C. (2009), Transport slopes, sediment cover, and bedrock channel incision in the Henry Mountains, Utah. *Journal of Geophysical Research, 114*(F2). doi:10.1029/2007jf000862

19) Lawrence,S. (2009). Fluvial Hydraulics. New York, NY: Oxford.

20) Limaye, A. B. S., & Lamb, M. P. (2016). Numerical model predictions of autogenic fluvial terraces and comparison to climate change expectations. *Journal of Geophysical Research: Earth Surface, 121*(3), 512-544. doi:10.1002/2014jf003392

21) Limaye, Ajay B. S. and Lamb, Michael P. (2014) *Numerical simulations of bedrock valley evolution by meandering rivers with variable bank material. Journal of Geophysical Research. Earth Surface*, 119 (4). pp. 927-950.

22) Meyer-Peter, E., and Muller R. (1948), Formulas for bed-load transport Proceedings of the International Association for Hydraulic Research, *Third Annual Conference, Stockholm, Sweden*, pp, 39-64.

23) Molnar, P., Erik Thorson, B., Burchfi el, B.C., Deng, Q., Feng, X., Li, J., Raisbeck, G.M., Shi, J., Zhangming, W., Yiou, F., and You, H., (1994), Quaternary climate change and the formation of river terraces across growing anticlines on the north flank of the Tien Shan, China: Journal of Geology, v. 102, p. 583–602, doi: 10.1086/629700.

24) Montgomery, D. R (2004), Observations on the role of lithology in strath terrace formation and bedrock channel width, *Am. J. Sci.*, Vol. 304, pp. 454–476.

25) Mosselman, E. and Crosato, A. (1991), `Universal bank erosion coefficient for meandering rivers (discussion)', J. Hydraul. Engng, 117, 942-943.

26) Nelson, P. A., Bolla Pittaluga, M., & Seminara, G. (2014). Finite amplitude bars in mixed bedrock-alluvial channels. *Journal of Geophysical Research: Earth Surface, 119*(3), 566-587. doi:10.1002/2013jf002957.

27) Schuurman, F., W. A. Marra, and M. G. Kleinhans (2013), Physics-based modeling of large braided sand-bed rivers: Bar pattern formation, dynamics, and sensitivity, *J. Geophys. Res. Earth Surf.*, 118, 2509–2527, doi:10.1002/2013JF002896.

28) Seidl, M. A., and Dietrich W. E (1992), The problem of channel erosion into bedrock, in Functional Geomorphology, *Catena Suppl.*, Vol. 23,edited by K. H. Schmidt and J. de Ploey, pp. 101–124.

29) Sklar, L. S. and W. E. Dietrich, (2001), Sediment and rock strength controls on river incision into bedrock, Geology [Boulder], 29[12], 1087-1090.

30) Sklar, L. S., Dietrich, W. E., Foufoula-Georgiou, E., Lashermes, B., & Bellugi, D. (2006). Do gravel bed river size distributions record channel network structure? *Water Resources Research, 42*(6), n/a-n/a. doi:10.1029/2006wr005035

31) Sklar, L. S., & Dietrich, W. E. (2004), A mechanistic model for river incision into bedrock by saltating bed load. *Water Resources Research, 40*(6), n/a-n/a. doi:10.1029/2003wr002496

32) Stark, C. P. (2006). A self-regulating model of bedrock river channel geometry. *Geophysical Research Letters, 33*(4). doi:10.1029/2005gl023193

33) Stock, J. D., Montgomery, D. R., Collins, B. D., Dietrich, W. E., & Sklar, L. (2005), Field measurements of incision rates following bedrock exposure: Implications for process controls on the long profiles of valleys cut by rivers and debris flows. *Geological Society of America Bulletin, 117*(1), 174. doi:10.1130/b25560.1

34) Stock, J. D., & Montgomery, D. R. (1999), Geologic constraints on bedrock river incision using the stream power law. *Journal of Geophysical Research: Solid Earth, 104*(B3), 4983-4993. doi:10.1029/98jb02139

35) Whipple, K. X. (2002). Implications of sediment-flux-dependent river incision models for landscape evolution. *Journal of Geophysical Research, 107*(B2). doi:10.1029/2000jb000044

36) Whipple, K. X., G. Hancock, and R. Anderson (2000), River incision into Bedrock: Mechanics and relative efficacy of plucking, abrasion, and cavitation, Geol. Soc. Am. Bull., 112, 490–503, doi:10.1130/0016-7606 [2000]112<490:RIIBMA>2.0.CO;2.

37) Whipple, K. X., & Tucker, G. E. (1999). Dynamics of the stream-power river incision model: Implications for height limits of mountain ranges, landscape response timescales, and research needs. *Journal of Geophysical Research: Solid Earth, 104*(B8), 17661-17674. doi:10.1029/1999jb900120

38) Zolezzi, G., Guala, M., Termini, D., & Seminara, G. (2005), Experimental observations of upstream overdeepening. *Journal of Fluid Mechanics, 531*, 191-219. doi: 10.1017/S0022112005003927.

Chapter 3

Sine Generated Curve Laboratory Scale Experiments: Lateral and Vertical Erosion in alluvial covered Incised Meander

The scarce knowledge of bedrock channel morphology has limited our understanding of landscape formation. Bedrock channel's morphology is controlled by various factors like sediment properties, climatic conditions, rock strength and local topography. In this study, laboratory scale experiments were conducted to understand the relationship between sediment feed rate and lateral erosion.

3.1 Introduction

Bedrock channel geometry has been believed to have advanced in the direction of a distinctive steady state configuration, in which the vertical erosion rate equals the rate of rock uplift or base level (Stark 2006, Wobus et al. 2006). This steady state is likely to be established in stimulus of local boundary conditions. These local boundary conditions have been divided into four broad classes as follows (Turowski et al. 2009): Climate and discharge conditions (Stark 2006), Substrate properties (Montgomery 2004) – The extent of bed and bank erosion would depend on factors like rock strength , River sediment load (Hancock and Anderson 1998) – Sediment load comprising the extent and inconsistency of sediment supply and its grain size distribution, Tectonic forcing (Harbor 1998)- An uplift or deformation in the land can force bedrock channels to change shape.

A majority of the research so far has focused all its attention towards exploring the effect of vertical erosion in bedrock meanders. To increase our understanding of processes effecting the formation of bedrock meanders, we need to understand the effect of lateral erosion in bedrock meanders. Lateral bedrock wearing down has sufficient proof and support of in field studies (Seidl and Dietrich 1992). Strath terraces that can be often observed in field provide a confirmation of how banks of bedrock evolve when lateral erosion is dominant over vertical erosion. Studies have revealed that lateral erosion was driven by sediment supply and high flow events (Turowski et al 2008). A couple of investigations suggest that high sediment supply forces lateral erosion over vertical erosion (Fuller et al 2009, Finnegan and Balco 2013). Nonetheless, all these studies fail to describe a specific mechanism leading into lateral wear off of bedrocks. In this study an attempt has been made to get a clear insight of relationship between sediment supply and erosion in bedrock channel.

3.2. METHODOLOGY

3.2.1 Particulars of experimental condition

A laboratory scale experiment was carried out to understand the interaction between sediment and banks of a bedrock channel. The experiments were performed at laboratory of Civil Engineering Research Institute for Cold Region (CERI) in Sapporo, Japan. A flume shaped of Sine Generated Curve was constructed, as shown in **Figure. 3.1**. The flume majorly consisted of weak mortar. It consisted of erodible bed and bank. The length of the flume was 3 meters and width was 5 cm. The banks of flume were 10 cm high. A small width flume was used to closely observe the effect of sediment on banks of flume. Water discharge rate, channel slope, sediment feed rate, and bed load grain size were kept constant throughout the experiment. The bed was covered initially with sediment. The initial alluvial thickness for bed was 0.5 cm. The sediment used as an alluvial cover for bed was the same size as the sediment supplied as load. The sediment supplied as a bed load had a very narrow size distribution with a median grain size of 0.75 mm. The diameter size of sediment and discharge were set such that, the sediment does not suspend in water. Slope of the flume was 0.01 and water was supplied at the rate of $5*10^{-4}$ m^3/second. The experiment never reached bank full condition. The experiment was conducted for 4 hours. A more detailed information about experimental conditions is provided in **Table 3.1**.

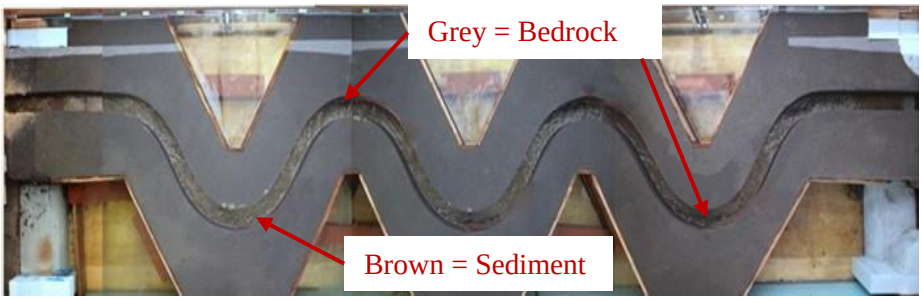

Figure 3.1 Experimental flume. The grey (dark) region in the flume is the exposed bedrock whereas the brown (lighter) region shows the alluvial deposit.

Initial alluvial thickness	0.5 cm
Grain diameter size	0.74mm
Wavelength	100cm
Slope	0.01
Water discharge	$0.0005 m^3/s$
Meander angle	60 degree
Bank Height	10cm
Channel Width	5cm
Time	4 hours
τ_*	0.122
Initial τ_{*c}	0.045

Table 3.1: Experimental Conditions

3.2.2 Experimental data collection procedure

The bank erosion width caused due to abrasion of bed load to the banks of bedrock channel was measured after 4 hours of the experiment. After the experiment was over, the flume was left to dry. Once dried, the sediment cover was removed carefully. A mixture of plaster of Paris (POP) was used to create a mould of the flume as shown in **Figure. 3.2(a)**. Once the mould was dry it was taken out by cutting the flume. The mould of flume is lateral and vertical inversion of the flume, i.e. the bank erosion width protrudes out in mould, shown explicitly in **Figure. 3.2(b)**. The pic shows the outer bend of the Curve 2. The red mark on Curve 2 in **Figure 3.2(a)** shows the part of flume which is used in the photo. The camera in **Figure 3.2(a)** shows the location from which photo is taken. The orange arrow in the **Figure 3.2(b)** shows the bank erosion in the flume. The mould of the flume is taken after removal of the sediment from the flume. The protruding portion shows the bank erosion (Definition of bank erosion is explained in **Figure 3.3**). The width of lateral erosion on left as well as right bank was obtained using a measuring tape. It was made sure that bank erosion caused due to sediment was only taken into account and that bank erosion caused due to water stream was not measured. The erosion caused due to sediment was 2 orders higher in depth as compared to erosion caused by water stream. Also, as our sediment was bed load only, bank erosion due to abrading sediment was limited to areas closer to bed**.** Water level was measured during the experiment using a point gauge.

3.3. RESULTS AND DISCUSSION

For ease of understanding, as well as in order to get critically accurate comparisons, the flumes have been divided, both for experiment and simulation into five imaginary parts, labelled as curve 1 to curve 5, as shown in **Figure. 3.2a**.

In laboratory experiments it was observed that, bed elevation increased in first curve especially near the inner bend. This indicates that sediment got deposited, especially in

the inner bend. As sediment got deposited in the inner bend, more sediment was forced to flow towards the outer bank leading into bank erosion due to abrasion. As sediment got deposited in curves near upstream, lesser sediment flowed towards the downstream curve. The downstream curve or Curve 5 witnessed very less, almost negligible bank erosion as sediment supply towards the downstream end was less. Curve 5 also witnessed an exposed bedrock bed due to lack of sediment supply.

Figure 3.3 shows the distance between upstream of the flume and the point of maximum erosion depth in a curve. **Figure 3.4** shows erosion in left and right banks of the flume. It shows how erosion is restricted to the outer bend only, as sediment was deposited in the inner bends.

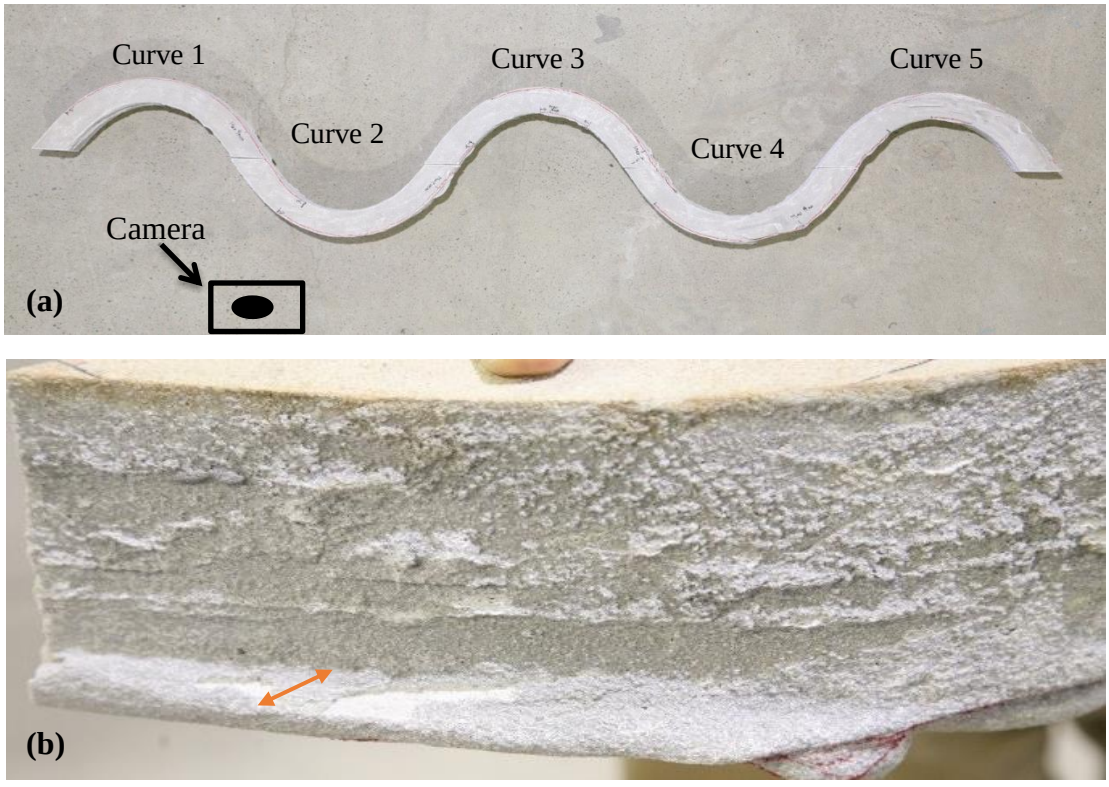

Figure. 3.2(a) Mould of the flume (b) Picture of mould showing bank erosion in the flume marked with an arrow

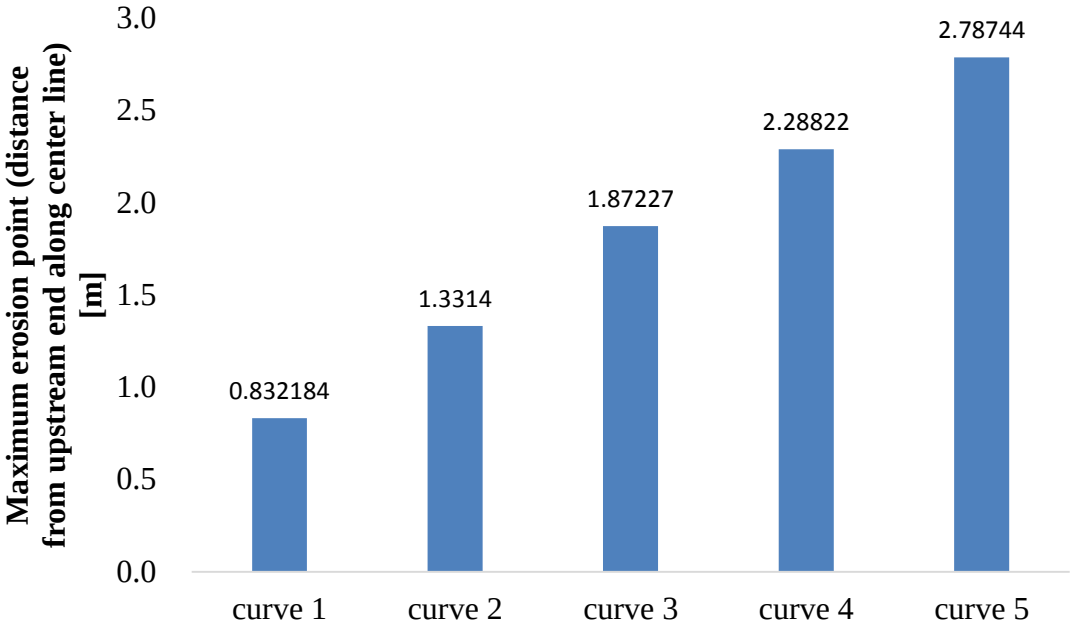

Figure 3.3 Graph showing the distance between upstream end and the location of maximum eroded point in a curve.

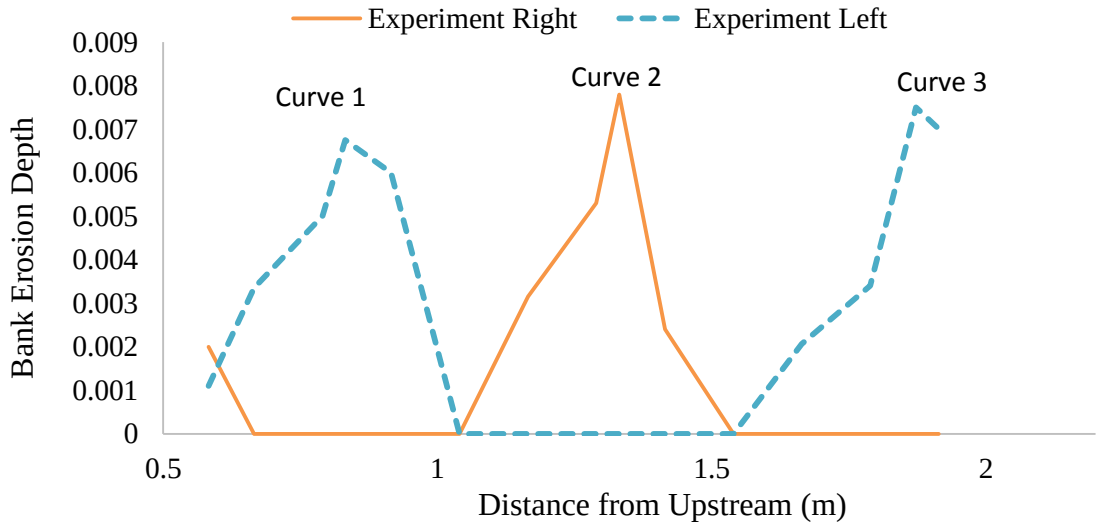

Figure 3.4 Graph showing erosion in left and right bank of the flume

3.4. CONCLUSIONS

In this study, laboratory experiments show that the sediment supply can cause abrasion in banks of bedrock channels. In the above mentioned experiment, the bank erosion occurred primarily due to bed load abrasion. This shows that sediment supply can be one of the dominant factors causing lateral erosion in bedrock meander.

REFERENCES

1) Stark, C. P.: A self-regulating model of bedrock river channel geometry, *Geophys. Res. Lett*., Vol. 33, pp. L04402, 2006.

2) Wobus, C. W., Tucker G. E., and Anderson R. S.: Self-formed bedrock channels*, Geophys. Res. Lett*., Vol. 33, pp. L18408, 2006.

3) Turowski, J. M., Lague D., and Hovius N.: Response of bedrock channel width to tectonic forcing: Insights from a numerical model, theoretical considerations, and comparison with field data, *J. Geophys. Res.,* Vol. 114, pp. F03016, 2009.

4) Montgomery, D. R.: Observations on the role of lithology in strath terrace formation and bedrock channel width, *Am. J. Sci.,* Vol. 304, pp. 454–476, 2004.

5) Hancock, G., and Anderson R. S.: Numerical modeling of fluvial strath terrace formation in response to oscillating climate, *Geol. Soc. Am. Bull*., Vol. 114, pp. 1131– 1142. 2002.

6) Harbor, D. J.: Dynamic equilibrium between an active uplift and the Sevier River, *Utah, J. Geol*., Vol. 106, pp. 181– 194, 1998.

7) Seidl, M. A., and Dietrich W. E.: The problem of channel erosion into bedrock, in Functional Geomorphology*, Catena Suppl.*, edited by K. H. Schmidt and J. de Ploey, Vol. 23,pp. 101–124, 1992.

8) Cook, K. L., Turowski J. M., and Hovius N.: River gorge eradication by downstream sweep erosion*, Nat. Geosci*., Vol. 7(9), pp. 682–686, 2014.

9) Turowski, J. M., Hovius N., Meng-Long H., Lague D., and Men-Chiang C.: Distribution of erosion across bedrock channels, *Earth Surf. Processes Landforms*, Vol. 33, pp. 353–363, 2008.

10) Fuller, T. K., Perg L. A., Willenbring J. K., and Lepper K.: Field evidence for climate-driven changes in sediment supply leading to strath terrace formation*, Geology*, Vol. 37(5), pp. 467–470,2009.

11) Finnegan, N. J., and Balco G.,: Sediment supply, base level, braiding, and bedrock river terrace formation*, Arroyo Seco, California, USA, Geol. Soc. Am. Bull*., Vol. 125(7-8), pp. 1114–1124, 2013.

Chapter 4

Numerical Simulations to Imitate Lateral Erosion in Bedrock Channels

In this study, a numerical model was implemented and tested to reproduce the lateral and vertical erosion in laboratory scale Bedrock meandering channels. The numerical model assumes that lateral erosion depends on an abrasion coefficient and transverse bedload transport rate per unit width. The numerical model could successfully trace lateral erosion in bedrock channels. Simulations were also performed to understand the effect of change in sediment supply on banks of bedrock channels. It can be seen from simulation results that sediment supply can be one of the dominating factors in determining the width of bedrock channels.

4.1 Introduction

Bedrock meanders take decades for their formation making it a daunting task to get field observation data. This gives rise to need of powerful numerical tools able to simulate the processes contributing to formation of a bedrock meander. Most of the previous bedrock channel evolution models use shear stress or stream power of water flow as the deciding factor for lateral erosion (Stark 2006, Wobus et al 2006). These models have helped us increase our understanding on how discharge, slope and tectonic activities impact width adjustment in bedrock channels. These models use shear stress/stream power erosion rule i.e., $E = k(\tau_b - \tau_{ce})a$, where E is bank erosion rate, τ_b signifies boundary shear stress, τ_{ce} represents critical shear stress for erosion, and k and a are constants. This model equation composes all relevant erosional processes into a single hydraulic parameter. These models ignored the effects of sediment transport in the channel. Some recent experiments and field studies have proposed sediment particle impact wear as a dominant factor for lateral erosion (Fuller et al 2016, Finnegan et al 2007).

In this study, an attempt had been made to implement a sediment and bank interaction proposed by Inoue et al (Inoue 2015). They assumed that the lateral erosion rate in bedrock depends on a multiplication of abrasion coefficient of bank with lateral bedload transport rate. This study also seeks to improve our understanding of effect of sediment supply rate on bank erosion. Simulations were performed with varying sediment supply to understand how it affected the width of bedrock. Also, some numerical calculations have been performed to observe the change in migration of bedrock channel in response to change in sediment cover and sediment feed rate.

4.2 Numerical Model

4.2.1 Flow model

The governing equations for a two-dimensional plane flow field are based on the numerical model proposed by Asahi et al (Asahi et al 2013). These equations are changed into a moving boundary-fitted coordinate (MBFC) system, but we write the equations here in an orthogonal coordinate system for simplicity.

In order to simulate 2 dimensional flow this model uses equation of continuity and equation of motion.

$$\frac{\partial h}{\partial t}+\frac{\partial (hu)}{\partial x}+\frac{\partial (hv)}{\partial y}=0 \tag{4.1}$$

$$\frac{\partial (uh)}{\partial t}+\frac{\partial \left(hu^2\right)}{\partial x}+\frac{\partial (huv)}{\partial y}=-gh\frac{\partial H}{\partial x}-\frac{\tau_x}{\rho}+D^x \tag{4.2a}$$

$$\frac{\partial (vh)}{\partial t}+\frac{\partial (huv)}{\partial x}+\frac{\partial \left(hv^2\right)}{\partial y}=-gh\frac{\partial H}{\partial y}-\frac{\tau_y}{\rho}+D^y \tag{4.2b}$$

in which

$$\frac{\tau_x}{\rho}=C_f u\sqrt{u^2+v^2} \tag{4.2a.a}$$

$$\frac{\tau_y}{\rho}=C_f v\sqrt{u^2+v^2} \tag{4.2b.a}$$

$$D^x=\frac{\partial}{\partial x}\left[\nu_t h\frac{\partial u}{\partial x}\right]+\frac{\partial}{\partial y}\left[\nu_t h\frac{\partial u}{\partial y}\right] \tag{4.2a.b}$$

$$D^y=\frac{\partial}{\partial x}\left[\nu_t h\frac{\partial v}{\partial x}\right]+\frac{\partial}{\partial y}\left[\nu_t h\frac{\partial v}{\partial y}\right] \tag{4.2b.b}$$

where h is the water depth, t is time, u and v represent velocity, g is gravitational acceleration, H is water level, C_f is a drag coefficient of shear stress, ν_t is an eddy viscosity coefficient calculated using Von Karman's coefficient ($\kappa = 0.4$) as :

$$v_t = \frac{\kappa}{6}(u_* h) \tag{4.2b.c}$$

where u_* is the shear velocity.

4.2.2 Bed friction

The friction of river bed is set using Manning's roughness parameter. The bed shear force is calculated using a drag coefficient of shear stress and Manning stickler equation as follows:

$$C_f = \frac{g}{h^{1/3}}\left(\frac{k_s^{1/6}}{7.66\sqrt{g}}\right) \tag{4.3}$$

k_s is hydraulic roughness height, calculated as $k_s=P_c k_a+(1-P_c)k_b$. Where k_a is alluvial roughness height (= $2d$), d is the diameter of grain, k_b is bedrock roughness height and P_c is the areal fraction of bed covered with sediment.

4.2.3 Sediment transport and conservation

The bedload transport capacity in this study is calculated using Meyer–Peter Müller formula (Meyer-Peter and Muller 1948). The bedload transport capacity of a channel is the maximum bedload transport rate, i.e. the maximum amount of bedload it can carry at a time, under given hydraulic conditions, maintaining a layer of alluvial deposit to provide cover effect.

$$q_{bc} = a_{qb}\left(\tau_* - \tau_{*c}\right)^{1.5}\sqrt{s_g g d^3} \tag{4.4}$$

where τ_* and τ_{*c} are dimensionless shear stress and dimensionless critical shear stress respectively. s_g is the specific weight of bed material in fluid and α_{qb} is a coefficient. The value of α_{qb} is 8, as given by Meyer-Peter Müller.

The dimensionless critical shear stress of mixed alluvial-bedrock bed is calculated from the following equation (Inoue et al 2014).

$$\tau_{*c} = 0.027\left(\frac{k_s}{d}\right)^{0.75} \tag{4.5}$$

The bedload transport rate is estimated from

$$q_b = \begin{cases} \dfrac{V_b}{V_{bc}} q_{bc} & for \quad 0 \le \dfrac{V_b}{V_{bc}} < 1 \\ q_{bc} & for \quad \dfrac{V_b}{V_{bc}} = 1 \end{cases} \tag{4.6}$$

here V_b is the volume of bedload per unit area and V_{bc} is the saturation volume of bedload per unit area (Inoue et al 2014). Following equation is used for sediment conservation (Inoue et al 2014, Luu et al 2004, Inoue et al 2016):

$$\frac{\partial V_b}{\partial t} + (1-\lambda)\frac{\partial \eta_a}{\partial t} + \left(\frac{\partial q_{b,x}}{\partial x} + \frac{\partial q_{b,y}}{\partial y}\right) = 0 \tag{4.7}$$

where η_a is the thickness of the alluvial layer. $q_{b,x}$, $q_{b,y}$ is vector of bedload transport rate per unit width. $q_{b,x}$, $q_{b,y}$ are estimated from the equations that consider the effect of secondary flow and the effect of local bed slope. In this numerical model, equations have been used in MBFC proposed by Watanabe et al. (Watanabe et al. 2001)

In **Eq. 4.7** when the thickness of η_a is 0, i.e. when bedrock is completely exposed $\partial\eta_a/\partial t$ also becomes 0 and V_b will vary from 0 to $V_{bc.}$ If V_b becomes larger than V_{bc}, sediment equal to (V_b - V_{bc}) deposits on the bed making the bed into a mixed alluvial channel. When alluvial thickness is equal to $\eta_{a,}$ i.e. bed is completely alluvial, sediment particles are exchanged between the alluvial layer and bedload layer making V_b= V_{bc}; hence in this situation, $\partial V_b/\partial t$ becomes 0.

4.2.4 Bedrock bed erosion

The vertical erosion rate of bedrock bed is calculated by following equation (Chatanantavet and Parker 2009)

$$\frac{\partial \eta_b}{\partial t} = -\beta_{bed}\sqrt{{q_{b,x}}^2 + {q_{b,y}}^2}\,(1-p_c) \tag{4.8}$$

where η_b is the elevation of bedrock layer, β_{bed} is the abrasion coefficient of the bed.

Following equation is used for the areal fraction of alluvial cover P_c.

$$p_C = \begin{cases} \eta_a / L & for \quad 0 < \eta_a < L \\ 1 & for \quad \eta_a \geq L \end{cases} \tag{4.9}$$

where L is bedrock macro roughness. When the bedrock surface is smooth, L is roughly $2d$.

4.2.5 Bedrock bank erosion

The saltating gravel particles strike riverbed under the influence of gravity, making the magnitude of bedload transport rate, one of the controlling factors for erosion rate of

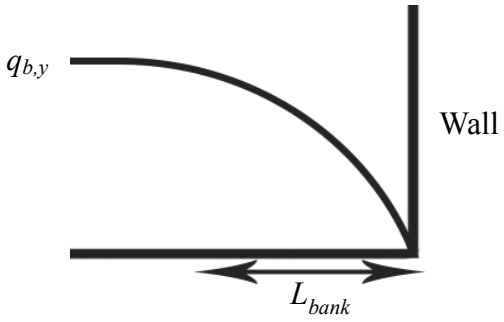

Figure.4.1 Definition of L_{bank}

bedrock bed (Sklar and Dietrich 2004). However, the erosion rate of bedrock bank not necessarily depends on the magnitude of bedload transport rate (Inoue 2015). For instance, in case of gravel moving parallel to the bedrock sidewall, the number of gravel hitting the sidewall is theoretically zero. The experimental result of Jagriti et al. (Jagriti et al 2016) showed that the bedrock bank erosion rate in straight channel is almost zero. Inoue assumed that the erosion rate of bedrock bank n_{bank} ($n_{b\text{-}right}$, $n_{b\text{-}left}$) depends on lateral bedload transport rate $q_{b,y}$ (Inoue 2015)

$$n_{b\_right} = -\beta_{bank}\, q_{b,y}\Big|_{y=L_{bank}} \tag{4.10a}$$

$$n_{b\_left} = \beta_{bank}\, q_{b,y}\Big|_{y=b-L_{bank}} \tag{4.10b}$$

where β_{bank} is the abrasion coefficient of the bank, $y = 0$ denotes the lateral position of the right bank, $y = b$ denotes the lateral position of the left bank. Lateral direction is the transverse direction of the channel. L_{bank} is an estimate of the distance of the boundary layer over which the transverse bedload rate decreases to zero at the bank, as shown explicitly in **Figure.4.1**. In our study, L_{bank} is taken as 10% of the channel width.

4.2.6 Effect of secondary flow

Effect of secondary flow for sediment transport was taken into consideration in this study. **Eq. 4.7** considers the effect of secondary flow on η_a, i.e. alluvial cover. **Eq. 4.9** involves the effect of secondary flow on P_c, calculated from **Eq. 4.7**. In order to maintain simplicity, effect of secondary flow on L_{bank} is not taken into consideration in presented model.

The model was implemented and tested by reproducing laboratory experiment. Simulations were performed with identical hydraulic conditions as laboratory experiment, shown explicitly in **Table 3.1** in Chapter 3.

Simulations were also performed to identify the effect of amount of sediment supplied on lateral erosion of bedrock channels. Simulations were performed with same hydraulic conditions as the laboratory experiment except that sediment feed rate was varied for each simulation as mentioned in **Table 4.1**.

Case 1.7 has a sediment feed rate of $1.7*10^{-5}m^2/s$, which is same as laboratory experiments. Case 1.7 represents the simulations performed to replicate laboratory experiments. Case 1 has a sediment feed rate of $1*10^{-5}m^2/s$. Names of cases represent the fraction of sediment feed rate, like Case 1.2 has a sediment feed rate of $1.2*10^{-5}m^2/s$, Case 1.5 has a sediment feed rate of $1.5*10^{-5}m^2/s$, Case 2 has a sediment feed rate of $2*10^{-5}m^2/s$ respectively. Increasing sediment has been fed from Case 1 to Case 2.

The bedrock hydraulic roughness of 0.008 was kept constant for all simulations. The bedrock hydraulic roughness was determined by trial and error method. It was determined so as to reproduce the water depth. Water depth increases with increase in bedrock hydraulic roughness. A constant bedrock bed erosion coefficient, i.e. β_{bed} of 0.1is used for all simulations. A bedrock bank abrasion coefficient β_{bank} of 2.5 was used for all simulations. The value of β_{bed} was determined by rock strength and equation proposed by Inoue et al (Inoue et al 2014) and β_{bank} was determined by trial and error method.

4.3 Calculation Condition

First, the laboratory scale experiments were reproduced. The cases use similar hydraulic condition as the Laboratory experiment. Calculations were also performed to see the effect of sediment supply on the formation and migration of Bedrock Meanders.

Cases	Sediment feed rate (m^2/sec)
Case 1	$1*10^{-5}$
Case 1.2	$1.2*10^{-5}$
Case 1.5	$1.5*10^{-5}$
Case 1.7	$1.7*10^{-5}$ (Same as lab experiments)
Case 2	$2*10^{-5}$

Table 4.1 Calculation Conditions

4.4 Simulations and discussion

4.4.1 Reproducing laboratory experiments.

Case 1.7 in simulation results is a replica of laboratory experiments. The bank erosion width in left and right banks of simulation results were compared with laboratory results, as shown in **Figure. 4.2**. It was found that the model could qualitatively and quantitatively reproduce the results. The model could trace the bank erosion, and mimic the behavior of erosion in left and right banks.

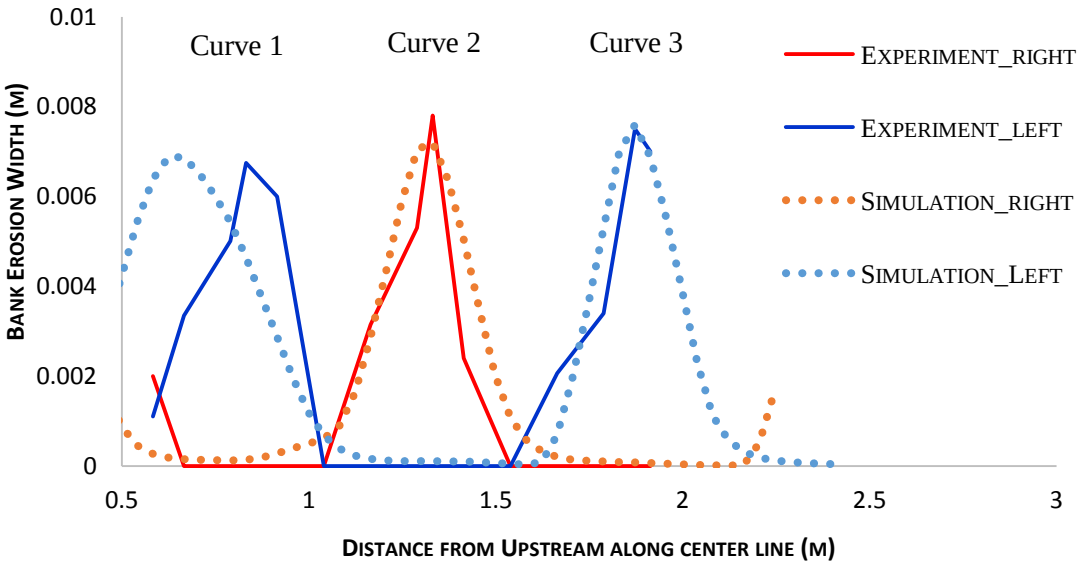

Figure.4.2 Comparison of bank erosion width in simulation results with laboratory experiment results.

The location of maximum bank erosion in simulations was compared with location of maximum bank erosion in experimental results, shown in **Figure. 4.3.** Location of maximum bank erosion is the point in a curve where maximum bank erosion occurred. The location of point with maximum bank erosion is measured along the center line of the flume. The simulation results show good agreement with experimental results. **Figure. 4.4** shows the counter map of areal fraction of alluvial cover (Pc in Eq. 5) in simulation results. The Curve 1 in simulation results is red, indicating the alluvial cover. The yellow or green color in simulation results represent exposed bedrock. The upstream end and inner bend tend to be covered with sediment. This tendency is in agreement with laboratory experiments (**Figure 3.1 in Chapter 3**).

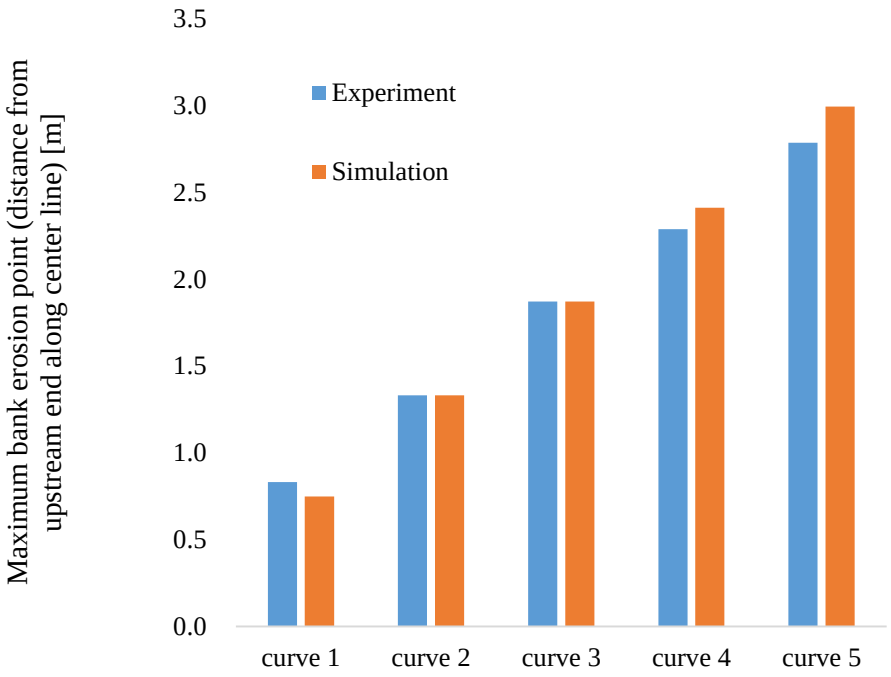

Figure.4.3. Comparison of location of maximum bank erosion depth, measured from upstream end.

4.4.2 Simulations to Identify Effect of Sediment Supply

The sediment supply was varied; keeping other hydraulic conditions same as in Case 1.7. In Case 1, when the sediment feed rate is $1*10^{-5}m^2/s$, the bedrock is exposed (represented by yellow color) in curve 1. As the sediment input is really low, the width of alluvial point bar becomes narrower than the channel width. Since very less sediment flowed towards the outer bend, the outer bend does not erode laterally.

As the sediment input was increased from Case 1 to Case 2, more sediment got deposited in the curves closer to upstream end (represented by red color). With increase

in sediment supply, the alluvial point bar got wider. With increase in width of alluvial point bar, more sediment flowed towards the outer bend leading into higher lateral erosion.

This relationship between sediment supply and lateral erosion is evident in **Figure. 4.5** where lateral erosion depth of Curve 1 and Curve 3 in each case is compared. An increase in erosion depth due to increasing sediment supply is prominent in Curve 1 than Curve 3. This happens as the effect of higher sediment decreases as the distance from the upstream end increases as a lot of sediment gets deposited in bends closer to upstream, decreasing the amount of sediment that can flow towards downstream end.

Also, the distance of location of maximum bank erosion in Curve 1 and Curve 3 of each case, was compared as shown in **Figure.4.6**. The distance between location of maximum bank erosion and location of bend apex is measured. In **Figure.4.6** it can be noticed that from Case 1 to Case 2, with increase in sediment feed rate the location of maximum bank erosion shifted closer to the upstream end. Higher sediment feed rate lead into migration of erosion location towards the upstream end. The effect of higher sediment feed rate cannot be noticed as lesser sediment flowed towards the downstream end and hence, tendency described above is remarkable in Curve 1 than Curve 3. This happened due to deposition of sediment. With increase in sediment supply, more sediment deposited in the inner bends. As the width of alluvial deposit increased, more sediment could reach the outer bend and abrade the banks.

Figure.4.7 represents the bedload flux of each case at the end of the simulation. It clearly demonstrates the shifting of bedload flux towards upstream of the channel with increase in sediment feed. The dark blue color represents less or no bedload flux. In Case 1, when sediment feed rate was really low, no bedload flux can be seen near the outer bends. Also, as shown in **Figure.4.7** the sediment collides with the outer bank at the downstream of the bend apex. As sediment feed rate is increased from Case 1 to Case 1.5, the bedload flux increases (represented by yellow or green color). As shown with the help of arrows, the bank erosion location shifted towards upstream of the channel.

Also, in Case 2, when sediment feed rate is maximum, most of the bedload travels towards the outer bend. Also, as shown in **Figure.4.7** the location of bank erosion shifts towards the upstream as sediment gets deposited in the inner bends increasing the amount of bedload that can flow towards the outer bend, also shifting the location towards the upstream.

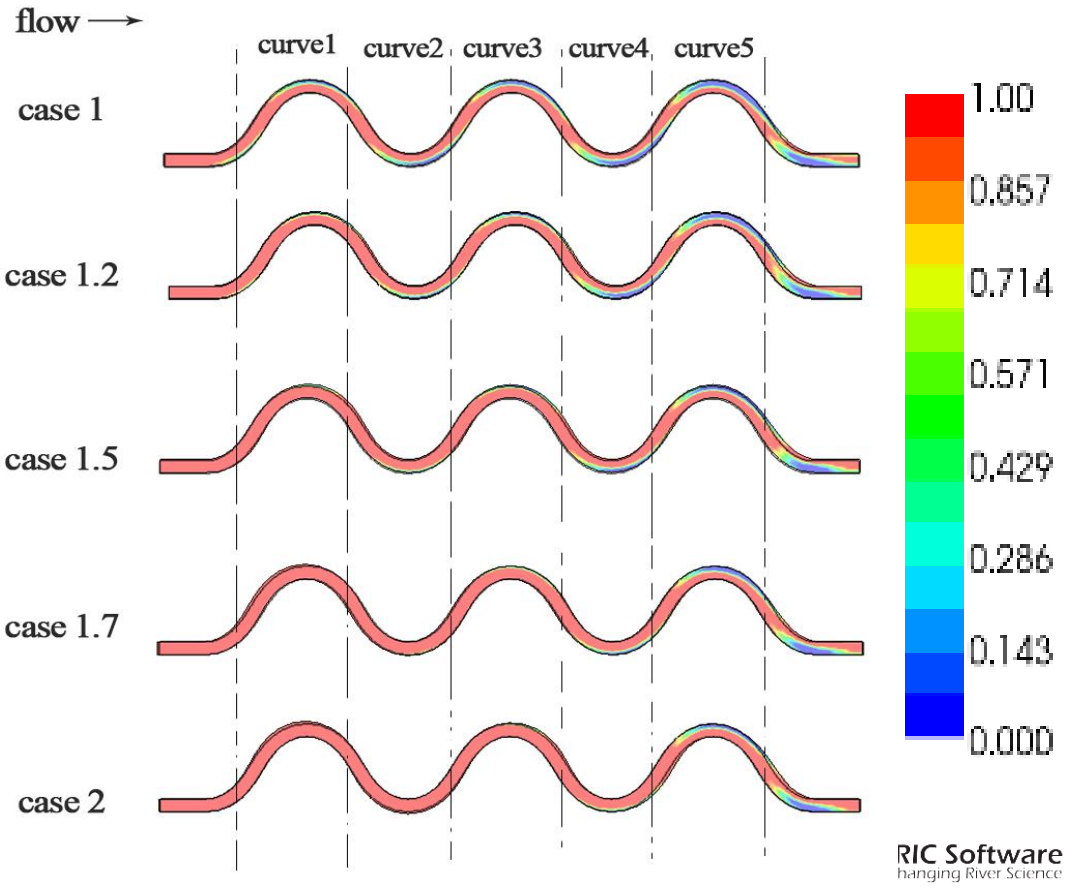

Figure.4.4 Simulation results showing dimensionless areal fraction of alluvial cover

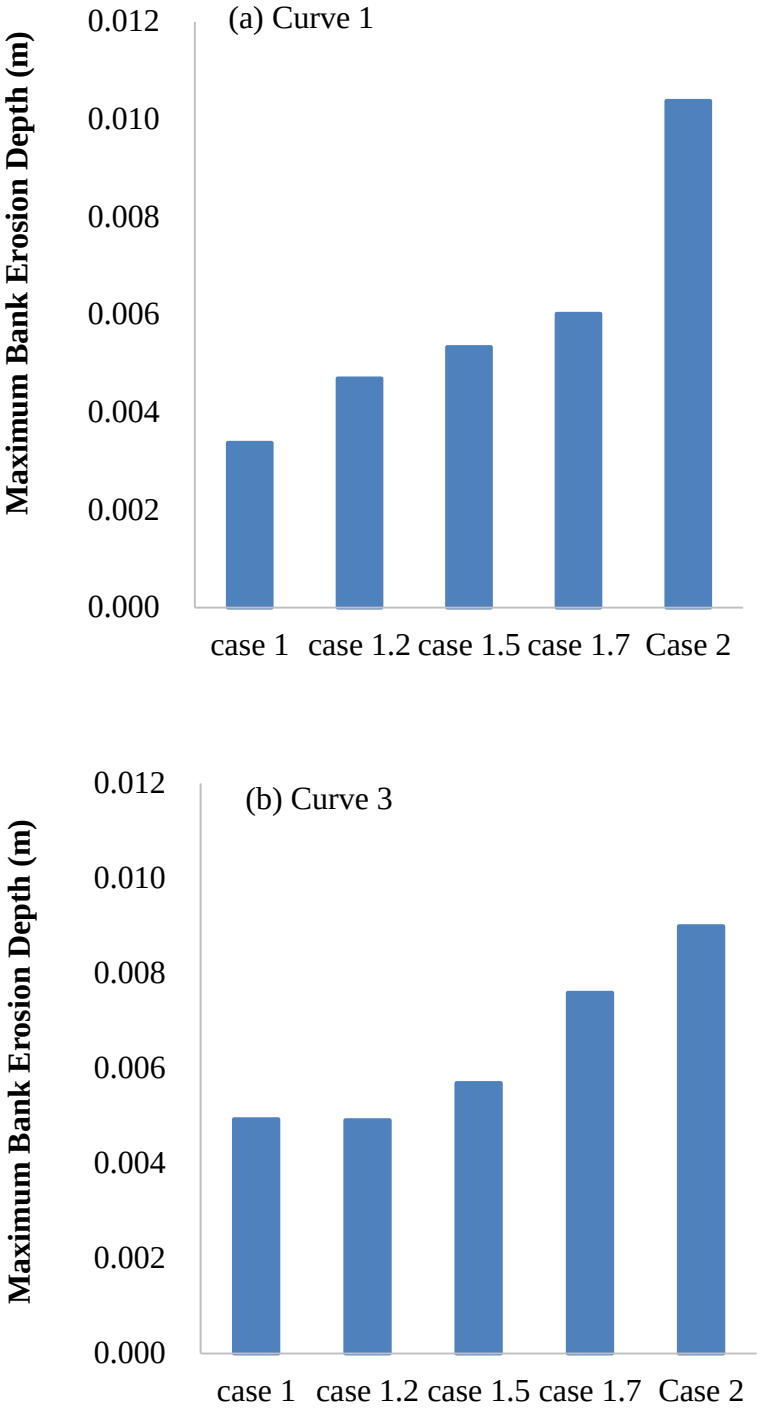

Figure 4.5. Effect of sediment feed rate in simulations. Comparison of bank erosion depth in (a) Curve 1 and (b) Curve 3. Sediment feed rate increases from Case 1 to Case 2.

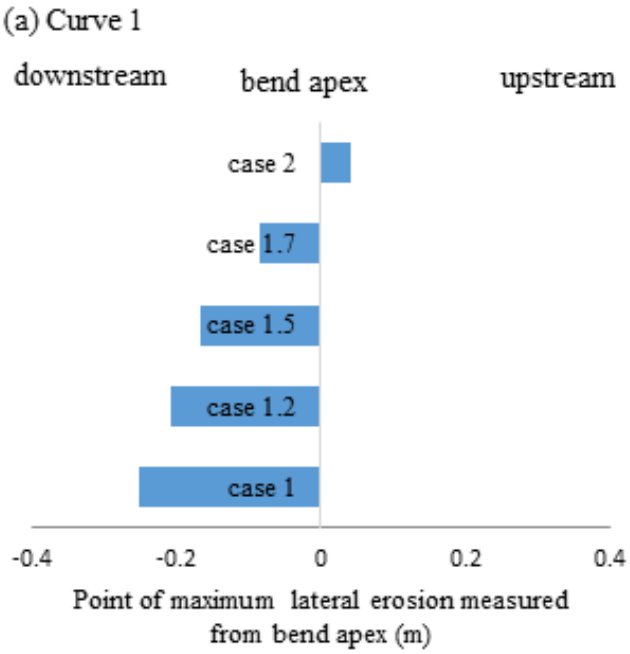

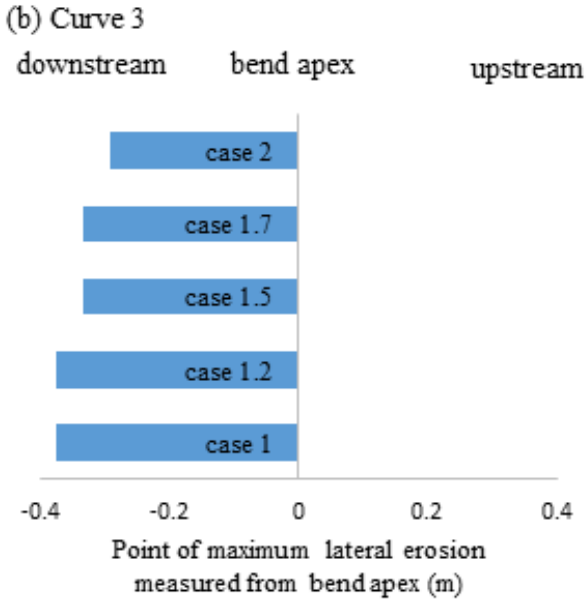

Figure 4.6. Effect of sediment feed rate. Comparison of point of maximum lateral erosion measured from bend apex in Simulation results. (a) Comparison results of curve 1 (b) comparison results of curve 3. Sediment feed rate increases from Case 1 to Case 2.

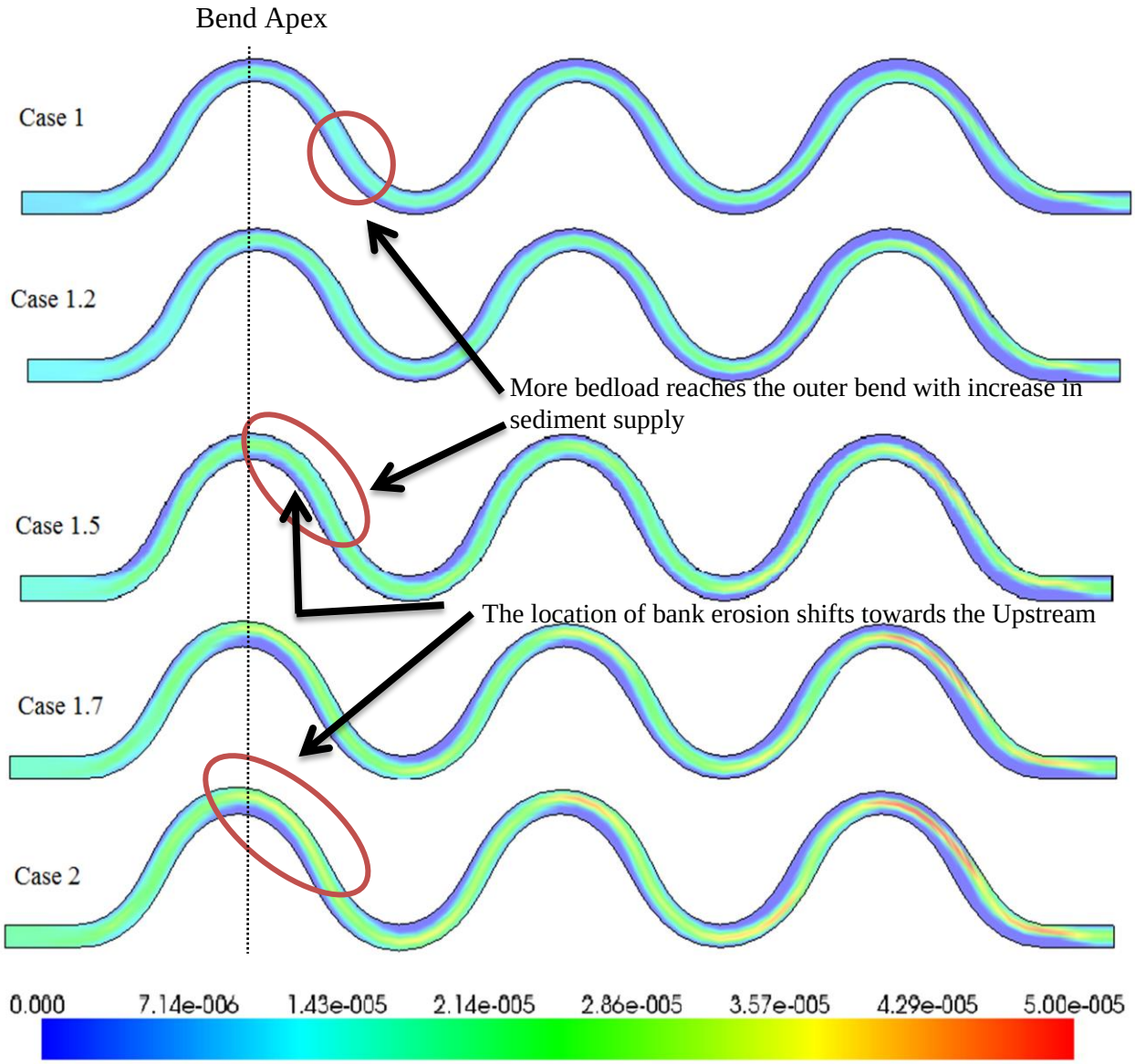

Figure 4.7. Bedload Flux in m^2/s. The bedload flux increases from case 1 to case 2 with increase in sediment feed rate. Location of bank erosion also shifts towards the Upstream.

4.5 Effect of Sediment Availability on Bedrock Channel

In order to observe how sediment cover affects the shape of bedrock meander, we performed 3 calculations using similar numerical conditions as mentioned in **Table 4.1**. The initial sediment cover thickness and sediment supply were varied in each case. A detail of sediment cover condition and sediment supply is provided in **Table 4.2**. The sediment cover decreases from Case 1 to Case 3. The water discharge, slope, meander angle, grain diameter size was used as mentioned in **Table 4.1**. Each simulation was run for 45,000 seconds.

We compared the water depth and alluvial cover of each case. We observed that, when initial alluvial cover is higher, as in Case 1, the outer banks of bedrock are eroded. Erosion of outer banks is shown explicitly in **Figure.4.2 Case1(a). Figure.4.2 Case1(a)** also shows the migration of bedrock meander from initial channel. Also, **Figure.4.2 Case1(b)** shows the areal fraction of alluvial cover in the channel. The bedrock channel is fully covered with alluvium deposits. The initial alluvial cover was decreased in Case 2 and as shown in **Figure.4.2 Case2(a)** erosion was observed in outer as well inner bank. Thin initial alluvial-thickness limit the sediment transport, especially in downstream section, thin point bar formation takes place in the inner bend, making inner bend prone to erosion. Also, the migration of bedrock meander was almost negligible towards the downstream of the channel. Due to a thin point bar formation, sediment cannot flow towards the outer bend, which eventually decreases the erosion in outer bends and hence the migration of channel is limited. In upstream section, enough sediment supply is given from upstream end, thick point bar is formed, making outer bend prone to erosion as shown in **Figure.4.2 Case2(b)**. In **Case 3**, the sediment cover and supply both are decreased, **Figure.4.2 Case3(a)** distinctly shows that there is no outer bank erosion in this case. Also, the meander doesn't migrate. Bedrock is only partially covered with alluvium as shown in **Figure.4.2 Case3(b)**. This happens because no or very thin point bar formation takes place when sediment supply is extremely low. As a result, flow is not sinuous forcing the flow and sediment hit the inner bank and eventually eroding the inner bank.

Case	Initial Sediment Cover (meter)	Sediment supply condition (m^2/s)
Case 1	0.01	$0.6*10^{-5}$
Case 2	0.005	$0.6*10^{-5}$
Case 3	0.005	$0.1*10^{-5}$

Table 4.2. Sediment cover thickness

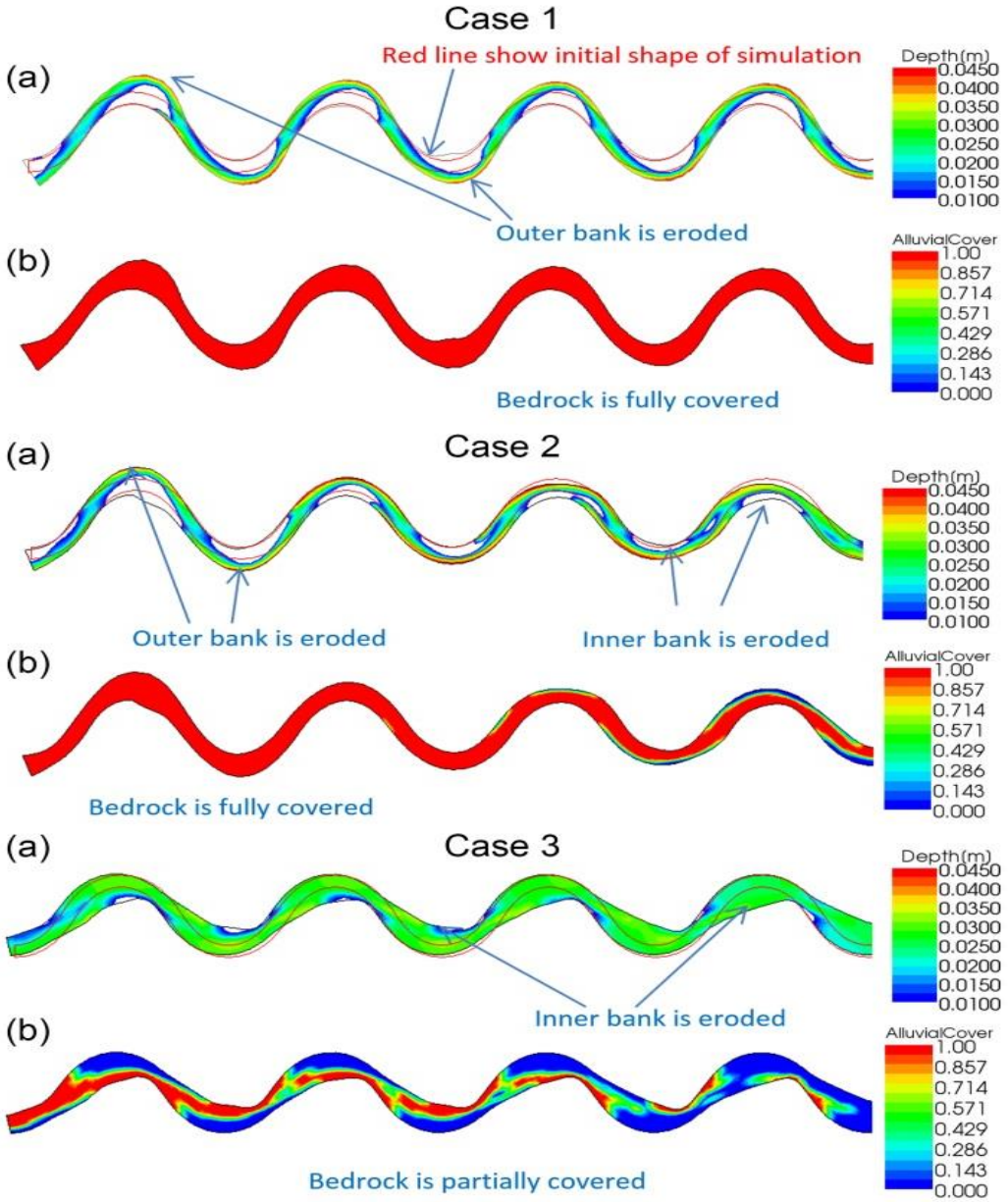

Figure 4.8: Effect of sediment on bedrock channel. Image (a) of each case shows water depth and image (b) of each case shows alluvial cover thickness

4.6 CONCLUSIONS

In this study, laboratory experiments show that the sediment supply can cause abrasion in banks of bedrock channels. In our experiment, the bank erosion occurred primarily due to bed load abrasion. This shows that sediment supply can be one of the dominant factors causing lateral erosion in bedrock meander

In this study, a model proposed by Inoue et al[5], has been implemented for simulating evolution of bedrock banks caused by sediment. The model could reproduce laboratory scale experiments quantitatively. However, in order to reproduce real river simulations, further improvements like taking into account the effect of suspended load will be required.

Simulations were performed to determine effect of sediment feed rate on lateral erosion. The results suggest that with increase in sediment feed rate, the magnitude of lateral erosion increased. The simulation results also suggest that increase in sediment feed rate, shifted lateral erosion closer to upstream end.

Also, simulations were performed to prove that bedrock meanders require sufficient alluvial cover and sediment supply for its formation. Sediment availability is a dominating factor in determining the shape of a bedrock meander.

References

1) Stark, C. P.: A self-regulating model of bedrock river channel geometry, *Geophys. Res. Lett*., Vol. 33, pp. L04402, 2006.

2) Wobus, C. W., Tucker G. E., and Anderson R. S.: Self-formed bedrock channels, *Geophys. Res. Lett*., Vol. 33, pp. L18408, 2006.

3) Fuller, T. K., Gran K. B., Sklar L. S., and Paola C.: Lateral erosion in an experimental bedrock channel: The influence of bed roughness on erosion by bed load impacts, J. Geophys.Res. Earth Surf.,Vol. 121,pp. 1084–1105, 2016.

4) Finnegan, N. J., Sklar L., and Fuller T. K.: Interplay of sediment supply, river incision, and channel morphology revealed by the transient evolution of an experimental bedrock channel, J. Geophys. Res.,Vol. 112,pp. F03S11, 2007.

5) Inoue, T: Numerical simulation of a bedrock-alluvial river bend that cuts downward and migrates laterally, both via incision, Gravel bed river 8, 2015.

6) Asahi, K., Y. Shimizu, J. Nelson, and G. Parker : Numerical simulation of river meandering with self-evolving banks, J. Geophys. Res. Earth Surf.,Vol. 118, pp. 2208–2229, 2013.

7) Meyer-Peter, E., and Muller R.: Formulas for bed-load transport Proceedings of the International Association for Hydraulic Research, Third Annual Conference, Stockholm, Sweden, pp, 39-64, 1948.

8) Inoue, T., Izumi N., Shimizu Y., and Parker G., Interaction among alluvial cover, bed roughness, and incision rate in purely bedrock and alluvial-bedrock channel, J. Geophys. Res. Earth Surf., Vol. 119, pp. 2123–2146, 2014.

9) Luu, L. X., S. Egashira and H. Takebayashi : Investigation of Tan Chau reach in lower Mekong using field data and numerical simulation, Annual Journal of Hydraulic Engineering, JSCE, Vol. 48, pp. 1057-1062, 2004.

10) Inoue, T., Iwasaki, T., Parker, G., Shimizu, Y., Izumi, N., Stark, C., and Funaki, J. : Numerical Simulation of Effects of Sediment Supply on Bedrock Channel Morphology, J. Hydraul. Eng.,Vol. 142,pp. 04016014, 2016.

11) Watanabe, A., Fukuoka, S., Yasutake, Y. and Kawaguchi, H. :Groin arrangements made of natural willows for reducing bed deformation in a curved channel, Advances on River Engineering, Vol. 7, pp. 285-290, (in Japanese), 2001

12) Chatanantavet, P. and Parker G.: Physically based modeling of bedrock incision by abrasion, plucking, and macroabrasion, J. Geophys. Res., Vol. 114, pp. F04018, 2009.

13) Sklar, L. S., and Dietrich W. E.: A mechanistic model for river incision into bedrock by saltating bedload, Water Resources Research, Vol. 40, pp. W06301, 2004.

14) Mishra J., Inoue T., and Shimizu Y.: Effect of bank erosion on bedrock sinuosity, IAHR APD, 2016.

15) Inoue, T. and Funaki, J. : Numerical Modeling of Riverbed Evolution in a Mixed Bedrock - Alluvial Channel, Monthly report of the Civil Engineering Research Institute, vol. 737, 2-9, 2014.

Chapter 5

Characteristic of Skewness in Meander Bends in Bedrock and Alluvial Channels

Understanding the differences between characteristics of alluvial and bedrock meanders is the need of hour. In this paper we have performed some numerical calculations in order to, first make an effort to observe the change in migration of bedrock channel in response to change in sediment cover and sediment feed rate. After realizing how sediment availability effects bedrock meanders, we tried to compare characteristics of alluvial and bedrock meanders under similar hydraulic and physical conditions.

5.1. INTRODUCTION

A very well-known meandering shape, often called as "Kinoshita type meandering" was first observed in Ishikari river of Japan. Kinoshita type meanders are asymmetric unlike sine generated curves. They are characterized by having multiple point bar growths in the inner bank of large-amplitude meander bends. Kinoshita type meanders are a common sight in alluvial rivers with high curvature and high amplitude bends (Parker et al. 1983, Parker and Andrews 1986, Kinoshita and Miwa 2009). **Figure.5.1** provides an insight to the shape of kinoshita meander, as marked by the square box, kinoshita meander's bend tilts towards the upstream.

During a field visit to a bedrock river, Shikaribetsu in Hokkaido region of Japan, we observed that the tilt of bend was towards the downstream of the upstream of river as shown in **Figure.5.2**. The characteristics of meandering in alluvial and bedrock channels are noticeably different from one another; the difference in tilt direction of bend is one such example.

Various attempts have been made in the past to understand alluvial rivers (Asahi et al. 2013, Parker et al. 2011). Despite various efforts to explore alluvial rivers, Kinoshita type meandering still lacks literature. Also, bedrock meanders haven't been studied and explored widely. A few attempts have been made to identify ways to distinguish between alluvial and Bedrock Rivers (Meshkova and Carling 2013). A broader understanding of differences in characteristics of alluvial and bedrock meanders is needed.

In this study, an attempt has been made to reproduce this difference in skewness observed in alluvial and bedrock channels. Also, it is explored, what conditions contribute to these differences. A 2 Dimensional model has been used to simulate this behavior of alluvial as well as Bedrock Rivers.

Figure.5.1 Kinoshita type meandering in Atlanta river, Alaska, USA. Image courtesy: Google Images

Figure.5.2 Meandering Shikaribetsu river. It is a bedrock river in Hokkaido, Japan. Image courtesy: Takuya Inoue

5.2. NUMERICAL MODEL

A 2-dimensional plane flow state is simulated by the basic equations of the numerical model for alluvial meanders presented by Asahi et al.(Asahi et al. 2013). Alluvial-layer deformation and sediment transport on bedrock channel are simulated by the system presented in Chapter 4 which is introduced by Inoue et al (Inoue et al 2014, Inoue et al 2016).

In numerical calculation system, the governing equations are changed into moving boundary-fitted coordinate system (Asahi et al. 2013), but we describe the equations in a curvilinear coordinate system for simplicity.

5.2.1 Alluvial bank erosion

This numerical model was implemented by Asahi et al (Asahi 2013) considering a

framework for modelling the migration of meandering rivers which was proposed by Parker et al (Parker et al. 2011). In a curvilinear coordinate system in **Figure.5.3**, the height of arbitrary position on the bank of alluvial river can be shown as

$$\text{right bank:} \quad Z_{BR} = Z_{BR}{}^{0} - \left(n - n_R{}^{0}\right)\tan\theta_{Bc} \tag{5.1}$$

$$\text{left bank:} \quad Z_{BL} = Z_{BL}{}^{0} + \left(n - n_L{}^{0}\right)\tan\theta_{Bc} \tag{5.2}$$

where $Z_{BR}{}^{0}$, $Z_{BL}{}^{0}$ are the height of bottom of bank, respectively. That is, these are the bed height at the connection point between bank and bed. $n_R{}^{0}$, $n_L{}^{0}$ are the axis values for $Z_{BR}{}^{0}$, $Z_{BL}{}^{0}$ in n direction. θ_{Bc} is the bank collapse angle. Alluvial bank shifting caused by bank erosion can be obtained by integrating Exner equation from bottom to top of the bank as mentioned below:

$$\frac{\partial n_R{}^{0}}{\partial t} = -\frac{1}{\tan\theta_{Bc}}\left[\frac{\partial Z_{BR}{}^{0}}{\partial t} + \frac{1}{1-\lambda}\left(\frac{\partial q_{bs}}{\partial s} + \frac{1}{B_R} q_{bn}\Big|_{n=n_R{}^{0}}\right)\right] \tag{5.3}$$

$$\frac{\partial n_L{}^{0}}{\partial t} = -\frac{1}{\tan\theta_{Bc}}\left[\frac{\partial Z_{BL}{}^{0}}{\partial t} + \frac{1}{1-\lambda}\left(\frac{\partial q_{bs}}{\partial s} + \frac{1}{B_L} q_{bn}\Big|_{n=n_L{}^{0}}\right)\right] \tag{5.4}$$

where, λ is porosity of bank material, B_R and B_L are the widths of right bank and left bank, respectively.

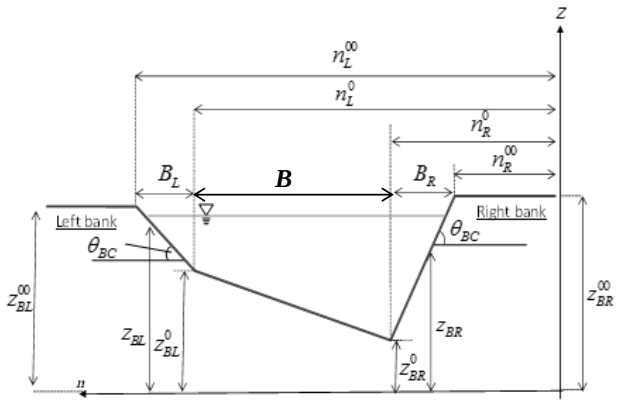

Figure.5.3 Variables used in river bank erosion model. (Courtesy: Asahi, 2014; thesis submitted to Hokkaido University)

5.2.2 Land accretion

Land accretion affects the shape of river over long time. Sediment deposition takes place on a point bar located at the convex part of the river. As time proceeds this area becomes higher. As this area is higher than channel, it rarely submerges. Vegetation can grow in this area. Vegetation works as a resistance to the stream, and catches fine sediment during flood; as a result the area's elevation grows up higher than before. With time, this area achieves the same height as the floodplain and it submerges only during floods (Asahi et al. 2013).

In estimating the amount of bank shift by land accretion, it is important to specify the area that rarely submerges. To specify this area, discharge, which indicates ordinary flow, was used in this model because it is hard to specify the area during flood. However, it is hard to assume that land accretion takes place at all of the specified area, as its progress depends on various factors (ex: sediment type, vegetation type, and climate). Relationship between those factors and land accretion phenomena is very complicated, and it takes long time to compute, so it is not treated in this study. So we defined a new parameter f_{land} which indicates a result of land accretion progress. If f_{land} is equal to 1, this means land accretion is occurring in all of the rarely submerged area. If f_{land} is equal to 0, this means that no land accretion occurred. When the water depth goes below minimum depth (h_{min}) and continues to stay below minimum water depth, the area is treated as dry. We cut the inner bank calculated as multiple of f_{land} with width of dry area. As it is difficult to define f_{land}, in this calculation f_{land} is set as 0.3 which is in accordance with Asahi's study (Asahi 2014).

5.3. NUMERICAL CONDITIONS

In this paper, we performed calculations to compare characteristics of alluvial and bedrock meanders. Initial channel width is 5cm. Bank height is 10 cm. Initial grid resolutions is 4.2cm (longitudinal direction) x 5 cm (transverse direction). B_R and B_L are same with transverse grid size. The hydraulic roughness is set as 2.5 times of grain size. The β_{bank} used in this study is 2.5, β_{bed} =1. All the numerical conditions are explicitly mentioned in **Table 1**.

Grain diameter size	0.74mm
Wavelength	100cm
Slope	0.01
Water discharge	$0.0005m^3/s$
Meander angle	60 degree
Bank Height	10cm

Table 5.1 Hydraulic Conditions

These are almost same with the conditions we used and succeeded to reproduce laboratory experiment of bedrock meander (Jagriti et al. 2016). And we also succeeded to reproduce an alluvial meander in sine-generated curve channel (Jagriti et al. 2015). In

this study, we perform a numerical experiment under the condition that validity of the model is confirmed to some extent.

5.4. RESULTS AND DISCUSSIONS

5.4.1 Comparing bedrock and alluvial meanders

In order to reproduce the differences in alluvial and bedrock meanders, we performed three calculations.

In **Figure.5.4(a)** it can be seen that the tilt in bend apex of alluvial bend is towards the upstream of the channel. This kind of meandering is famously known as kinoshita meander. Whereas, **Figure.5.4(b)** shows the meandering migration in bedrock channel. It is evident that the tilt in bend apex in bedrock bend is towards the downstream of the channel. **Figure.5.4(a)** does not provide a very clear appearance of tilt in the bend apex towards the upstream of alluvial channel. As this calculation inhibits inner bank accumulation, the calculations cannot be carried on for a longer duration of time because the calculations will fail due to grid shape strain caused by excessive bank erosion. Hence, in order to get much distinctive results for kinoshita alluvial meanders, we performed calculations with active bank accumulation system. **Figure.5.4(c)** indicates explicitly, the tilt of bend apex towards the upstream of alluvial channel. Similar behavior of alluvial and bedrock meanders were observed in real rivers, showed in aerial photographs of Atlanta river and Shikaribetsu river in **Figure. 5.1** and **Figure. 5.2** respectively.

Seminara (Seminara 2006) employed a linear model of flow and bed topography. They showed that meanders behave as linear oscillators. They resonate at some values of aspect ratio of channel and meander wavenumber. In this study, he suggested that downstream migration and upstream skewing (the tilt of bend apex towards the upstream) of meander patterns is obtained under sub-resonant conditions. Their results were in fair agreement with Kinoshita's (Kinoshita 1974) laboratory observations. And our results of alluvial meanders are consistent with his study. However, our results of bedrock meanders show downstream migration with downstream skewing (the tilt of bend apex towards the downstream). This may be an interesting phenomenon in a mixed bedrock-alluvial meandering channel.

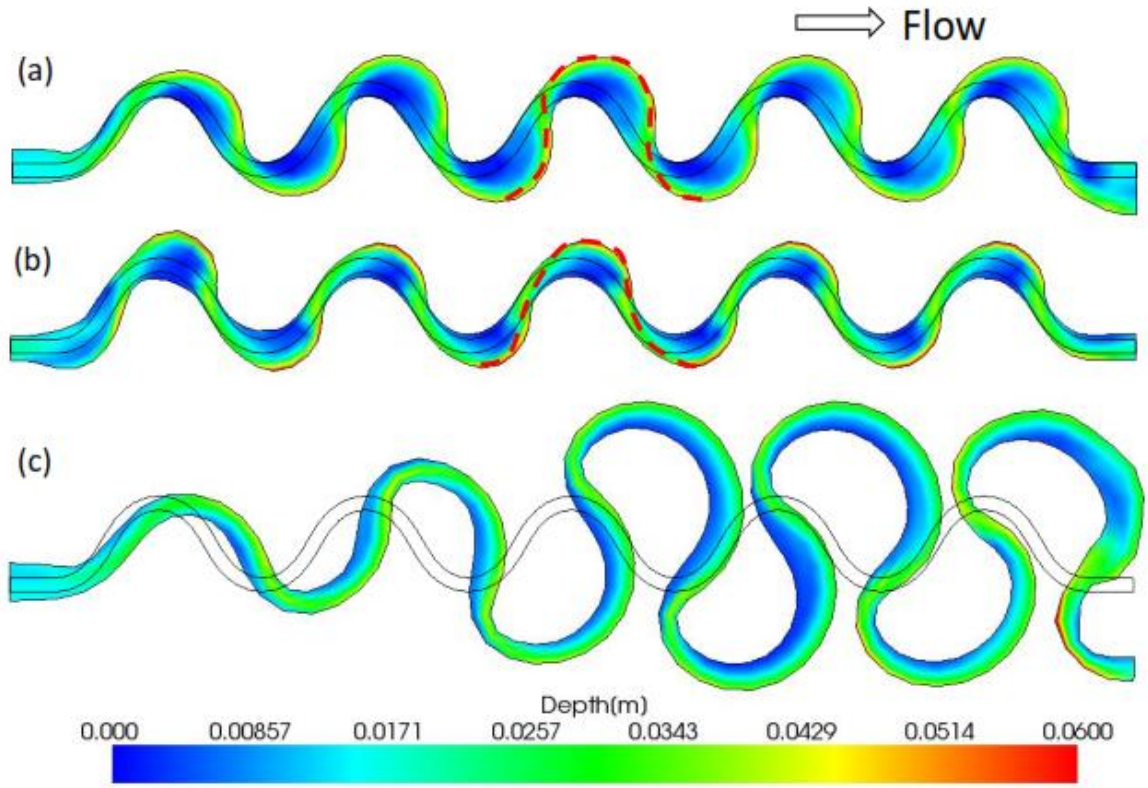

Figure.5.4 Meander bend migration. (a) Alluvial meander without bank accumulation (b) Bedrock meander without bank accumulation. (c) Alluvial meander with land accretion

5.4.2 Factors Affecting skewness in Bedrock Channel

In this section, an attempt has been made to discover the factors affecting downstream skewness in Bedrock meanders. Also, I tried to find out the natural wavelength of Bedrock meanders. Natural wavelength is the stable state that every river tries to achieve. Natural wavelength of Bedrock Rivers is examined here for different initial bed angles, keeping all other hydraulic conditions similar in each case.

5.4.2.1 Effect of Bed Angle

All the hydraulic conditions except bed angle is taken same as mentioned in **Table 5.1**. The bed angle is varied as mentioned in **Table 5.2**

Bed Angle	100 degree
	90 degree
	80 degree
	60 degree
	40 degree

Table 5.2 Bed Angles for finding natural wavelength and skewness of Bedrock Rivers

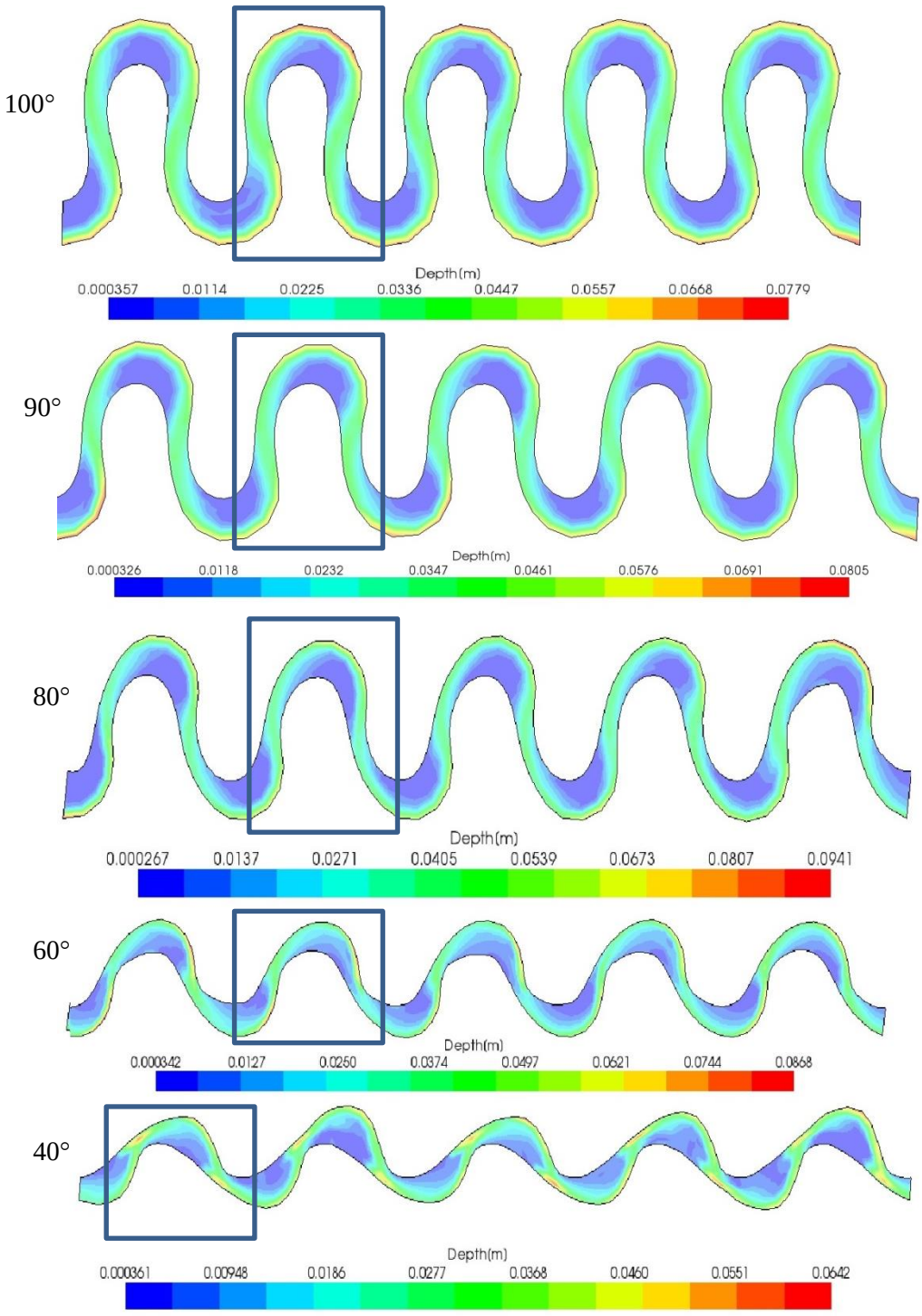

Figure 5.5 Skewness of Bedrock River is towards the downstream irrespective of the initial bed angle.

The skewness in bedrock remains downstream irrespective of the initial bed angle.

5.4.2.2 Effect of initial wavelength

Effect of initial wavelength was also studied in this thesis. The following table provides the details about the different calculations done by changing the wavelength. All other hydraulic conditions are kept similar, only wavelength is varied.

Wavelength	0.75m
	2m
	4m

Table 5.3 Initial Wavelength for finding natural wavelength and skewness of Bedrock Rivers

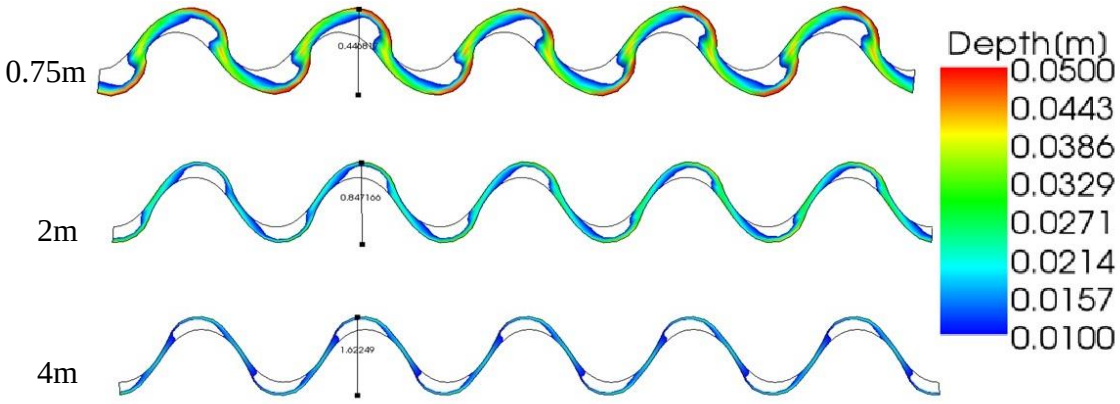

Figure 5.6 Skewness of Bedrock River is towards the downstream when initial wavelength is low (0.75m and 2m). The channel shows upstream migration when initial wavelength increases (4m)

Figure 5.6 shows that the direction of skewness is towards the downstream when wavelength is low, i.e. 0.75m and 2m. When the wavelength is high, the direction of skewness is towards Upstream. I tried to perform another calculation with a higher wavelength and higher resolution to get a clearer perspective of what could cause the skewness to shift towards upstream when initial wavelength is high.

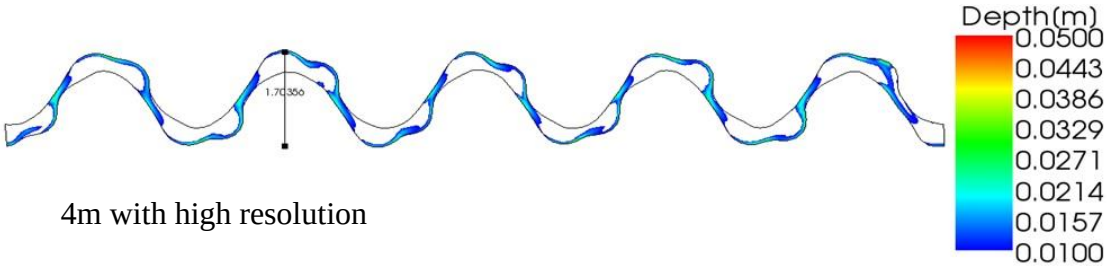

Figure 5.7 The number of wavenumber is increasing

In **Figure 5.7** it can be seen that the wavenumber is increasing. This might happen as bedrock channel tries to attain its natural wavelength. The natural wavelength of bedrock might be a low one ~1m-2m, and as the wavelength increases, the bedrock channel tries to attain its natural wavelength by creating new waves.

5.5 CONCLUSIONS

We successfully reproduced the characteristics of alluvial and bedrock meanders observed often in field. Alluvial meander's bend tends to tilt in the direction of upstream which is in contrast to Bedrock meanders, in which the bend tilts towards the downstream of the channel. Also, the study confirms that change in bed angle does not alter the skewness in Bedrock Meanders. Change in wavelength affects the skewness, when wavelength is low; the skewness is towards downstream whereas it is upstream when wavelength increases.

REFERENCES

1) Parker, G., Diplas, P and Akiyama, J.: Meander bends of high amplitude, *J. Hydraulic Eng.,* Vol. 109, Issue 10, pp. 1323-1337, 1983.

2) Parker, G. and Andrews, E.D. : On the time development of meanders bends, *J. Fluid Mech*., Vol. 162, pp. 139-156, 1986

3) Kinoshita, R. & Miwa, H.: River channel formation which prevents downstream translation of transverse bars (in Japanese) *Shinsabo*,Vol. 94, pp.12–17, 1974.

4) Asahi, K., Shimizu Y., Nelson J., and Parker G. : Numerical simulation of river meandering with self-evolving banks, *J. Geophysical Research:Earth Surface*, Vol. 118, pp. 2208-2229, 2013.

5) Parker, G., Shimizu Y., Wilkerson G.V., Eke E.C., Abad J.D, Lauer J.W., Paola C., Dietrich W.E. and Voller V.R.: A new framework for modeling the migration of meandering rivers, *Earth Surf. Processes Lanforms*, Vol. 36, issue 1, pp. 70-86, 2011.

6) Meshkova, L. V. and Carling, P. A.: Discrimination of alluvial and mixed bedrock–alluvial multichannel river networks, *Earth Surf. Process. Landforms,* Vol. 38, pp. 1299–1316, 2013.

7) Inoue, T., Izumi, N., Shimizu, Y., and Parker, G. : Interaction among alluvial cover, bed roughness, and incision rate in purely bedrock and alluvial-bedrock channel, *J. Geophys. Res. Earth Surf.,* 119, 2014.

8) Inoue, T., Iwasaki, T., Parker, G., Shimizu, Y., Izumi, N., Stark, C., and Funaki, J.: Numerical simulation of effects of sediment supply on bedrock channel morphology, *J. Hydraul. Eng.,* 2016.

9) Parker, G., Shimizu Y., Wilkerson G.V., Eke E.C., Abad J.D., Lauer J.W., Paola C., Dietrich W.E. and Voller V.R. A new framework for modeling the migration of meandering rivers, *Earth Surf. Processes Lanforms*, vol. 36, issue 1, pp. 70-86, 2011.

10) Asahi, K.: Numerical simulation of river meandering with self-evolving banks. *Thesis submitted to Hokkaido University.* (2014)

11) Jagriti M., Inoue T., and Shimizu Y.: Simulations of Lateral Erosion in Bedrock Channels, *Abstracts of Applied Mechanics*, 100077, 2016.

12) Jagriti M., Asahi K., Shimizu Y., and Parker G.. Numerical investigation of Channel evolution considering bank erosion and land accretion, *RCEM*, 2015.

13) Seminara, G. : Meanders, *J. Fluid Mech*, Vol. 554, pp. 271–297,2006.

Chapter 6

Summary and Future Work

6.1 Summary and Conclusions

This thesis is aimed at exploring the factors controlling the shape of meanders. In the first part of this thesis, an attempt has been made to understand the effect of sediment on shape of a bedrock meander.

First, laboratory scale experiments were conducted using U-Shaped bedrock bend channel. Various cases were performed by varying the sediment supply. These set of experiments proved that an increase in sediment supply accelerates bank erosion and inhibits bed erosion. Increased sediment flux also shifts start point of bank erosion towards the upstream. Additionally, it also increases the length as well as depth of the bank erosion in bedrock channels. The increased sediment flux also makes the effect of lateral bed slope dominate over the effect of secondary flow. These set of experiments also show that bedrock channel is dominantly eroded in the centre of the channel.

In order to get an even clearer perspective of how sediment affects the curves of bedrock, another set of laboratory scale experiments were performed using Sine Generated Curve channel. In these experiments it was observed that bed elevation increased in first curve of the Sine Generated Curve channel, i.e. upstream section of the channel. The effect of sediment was less in the downstream sections of the bend as most of the sediment got deposited in the upstream section.

The above experimental results aided in formation of relationship between sediment flux and bed and bank erosion in bedrock channel. The experiments performed during this thesis provide a cogent proof that magnitude alone is not solely responsible for erosion caused by bed load in bedrock channels. In cases when gravel moves parallel to the channel, the number of gravel hitting the sidewall is theoretically zero, unless roughness of bed is changed by introducing boulders in the bed. In case of flood or high sediment discharge, the bed gets covered with uniform roughness sediment. Inoue (2015) assumed that the erosion rate of bedrock bank depends on lateral bedload transport rate. In this study, this relationship is numerically modelled and tested for its accuracy. The proposed numerical method could trace the erosion rate in laboratory

scale experiments.

Numerical simulations were also performed to identify the effect of sediment supply on curves of bedrock channel. The simulation results attest that with increase in sediment supply, the erosion rate increases. Additionally, it also proves that increase in sediment supply shifts lateral erosion closer to the upstream end.

Also, the proposed model could reproduce the on field characteristic for skewness in alluvial and bedrock meanders. The direction of skewness remains towards the downstream irrespective of the bed angle. When the initial wavelength is short, bedrock shows downstream skewness. When the initial wavelength is long, bedrock shows upstream skewness or change towards a natural wavelength.

6.2 Future Work

Although, the model presented in this study can successfully trace bank and bed erosion in bedrock meanders, the sediment supply and rock strength of bedrock banks dominantly affects the erosion rate in bedrock meanders. Especially in colder regions like Hokkaido, where rivers often suffer from freezing temperatures, followed by thawing seasons, the rock strength of bedrock is severely affected by the freeze-thaw cycles it goes through. The present model cannot calculate the effect of freeze-thaw cycles on bedrock channels.

Even though, freeze-thaw is a common phenomena effecting river channels in colder region, there is a scarcity in literature explaining its consequences. Presently, there is no efficient model which can deal with freeze-thaw weathering cycles. Several past studies have increased our understanding of relationship between porosity and sediment production due to freeze thaw (Izumiyama et al.,Kyoto Univ, 2012; Matsuoka et al. ESPL,2001). Previous model can estimate the amount of sediment production due to freeze-thaw (Tsutsumi and Fujita, Geomorphology, Vol. 267, 2016). One can extend these studies to understand the effect of freeze-thaw on rate of bank and bed erosion.

Various observations have suggested that freeze-thaw cycles make the bed and banks of bedrock channels weaker by creating void and expansion in it. When water enters the cracks in beds and banks and freezes, its volume increases by nearly 10%, which can exert a pressure of up to 21 mega Pascals on the rocks. When the ice thaws, it flow

further deep into the rock cracks and freezes again, making the rock weaker and prone to weathering and abrasion by saltating bedload. Often, very commonly observed erosion caused by freeze-thaw cycles is formation of scree slopes or talus slopes. These cycles of freeze and thaw severely control the erosion rate and channel morphology in Bedrock channels. According to a previous study, strength of rock changes linearly with the number of freeze-thaw cycles (Kusakabe and Ito, 2015,JSCE, Vol.71,47-54).

I suggest to explore the effect of freeze-thaw weathering on channel bank and bed erosion rate and enhance our current model to enable it to deal with the effect of freeze-thaw cycles; and be able to trace and reproduce bed and bank erosion influenced by weakened frozen-thawed rocks.